



HAL
open science

Stretch Factor of Long Paths in a planar Poisson-Delaunay Triangulation

Nicolas Chenavier, Olivier Devillers

► **To cite this version:**

Nicolas Chenavier, Olivier Devillers. Stretch Factor of Long Paths in a planar Poisson-Delaunay Triangulation. [Research Report] RR-8935, Inria. 2016, pp.34. hal-01346203

HAL Id: hal-01346203

<https://inria.hal.science/hal-01346203>

Submitted on 18 Jul 2016

HAL is a multi-disciplinary open access archive for the deposit and dissemination of scientific research documents, whether they are published or not. The documents may come from teaching and research institutions in France or abroad, or from public or private research centers.

L'archive ouverte pluridisciplinaire **HAL**, est destinée au dépôt et à la diffusion de documents scientifiques de niveau recherche, publiés ou non, émanant des établissements d'enseignement et de recherche français ou étrangers, des laboratoires publics ou privés.

Inria

Stretch Factor of Long Paths in a planar Poisson-Delaunay Triangulation

Nicolas Chenavier, Olivier Devillers

**RESEARCH
REPORT**

N° 8935

July 2016

Project-Team Vegas

ISRN INRIA/RR--8935--FR+ENG

ISSN 0249-6399



Stretch Factor of Long Paths in a planar Poisson-Delaunay Triangulation

Nicolas Chenavier*, Olivier Devillers^{†‡§}

Project-Team Vegas

Research Report n° 8935 — July 2016 — 34 pages

Abstract: Let $X := X_n \cup \{(0, 0), (1, 0)\}$, where X_n is a planar Poisson point process of intensity n . We prove that the distance between the expected length of the shortest path between $(0, 0)$ and $(1, 0)$ in the Delaunay triangulation associated with X belongs to $[1 + 2.47 \cdot 10^{-11}, 1.182]$ when the intensity of X_n goes to infinity. Experimental values indicate that the correct value is about 1.04. We also prove that the expected number of Delaunay edges crossed by the line segment $[(0, 0), (1, 0)]$ is $\frac{64}{3\pi^2} \sqrt{n} + O(1) \simeq 2.16\sqrt{n}$.

Key-words: Probabilistic analysis – Worst-case analysis – Walking algorithms

Part of this work is supported by: ANR blanc PRESAGE (ANR-11-BS02-003).

* Université du Littoral Côte d'Opale, France. nicolas-chenavier.fr/

† Inria, Centre de recherche Nancy - Grand Est, France.

‡ CNRS, Loria, France.

§ Université de Lorraine, France

**RESEARCH CENTRE
NANCY – GRAND EST**

615 rue du Jardin Botanique
CS20101
54603 Villers-lès-Nancy Cedex

Bornes sur l'élongation du plus court chemin dans la triangulation de Delaunay d'un processus de Poisson de grande densité

Résumé : Soit $X := X_n \cup \{(0, 0), (1, 0)\}$, où X_n est un processus ponctuel de Poisson planaire d'intensité n . Nous montrons que la longueur du plus court chemin entre $(0, 0)$ et $(1, 0)$ dans la triangulation de Delaunay de X est dans l'intervalle $[1 + 2.47 \cdot 10^{-11}, 1.182]$ quand n tends vers l'infini. Les résultats expérimentaux indiquent que la valeur correcte est 1.04. Nous montrons aussi que l'espérance du nombre d'arêtes de Delaunay coupées par le segment $[(0, 0), (1, 0)]$ est $\frac{64}{3\pi^2}\sqrt{n} + O(1) \simeq 2.16\sqrt{n}$.

Mots-clés : Analyse probabiliste – Analyse dans le cas le pire – Algorithmes de marche

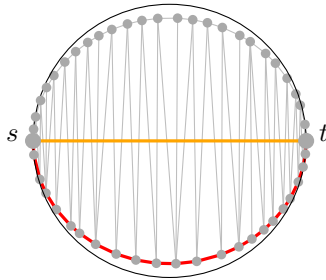


Figure 1: The shortest path in the Delaunay triangulation (red) can be about $\frac{\pi}{2}$ larger than the line segment (yellow).

1 Introduction

Let χ be a locally finite subset in \mathbb{R}^d , endowed with its Euclidean norm $\|\cdot\|$, such that each subset of size $n < d + 1$ are affinely independent and no $d + 2$ points lie on a sphere. If $d + 1$ points x_1, \dots, x_{d+1} of χ lie on a ball that contains no point of χ in its interior, we define an edge between x_i and x_j for each $1 \leq i \neq j \leq d + 1$. The set of these edges is denoted by $\text{Del}(\chi)$ and the graph $(\chi, \text{Del}(\chi))$ is the so-called Delaunay graph associated with χ [17, p. 478]. Delaunay triangulation is a very popular structure in computational geometry [1] and is extensively used in many areas such as surface reconstruction [5] or mesh generation [8].

In this paper, we investigate several paths in $\text{Del}(\chi)$. By a path $P = P(s, t)$ between two points $s, t \in \chi$, we mean a sequence of segments $[Z_0, Z_1], [Z_1, Z_2], \dots, [Z_{k-1}, Z_k]$, such that $Z_0 = s$, $Z_k = t$. In particular, we say that P is a path in $\text{Del}(\chi)$ if it is a path such that each segment $[Z_i, Z_{i+1}]$ is an edge in $\text{Del}(\chi)$. The investigation of paths is related to walking strategies which are commonly used to perform point location in planar triangulations [11] or routing in geometric networks [4]. One of the classical works concerns the so-called straight walk which deals with the set of triangles cut by the line segment $[s, t]$. In this context, Devroye, Lemaire and Moreau [12] consider n points evenly distributed in a convex domain and prove that the expected number of Delaunay edges crossed by a line segment of length L is $O(L\sqrt{n})$. This result is improved by Bose and Devroye [3] who show that the complexity equals $\Theta(\sqrt{n})$, even if the line segment depends on the distribution.

Another classical problem in walking strategies is the investigation of the stretch factor associated with two nodes $s, t \in \chi$ in $\text{Del}(\chi)$. This quantity is defined as $\frac{l(SP_\chi)}{\|s-t\|}$, where $l(SP_\chi)$ is the length of the shortest path between s and t . Many upper bounds were established for the stretch factor in the context of finite sets χ , e.g. [13, 16]. The best upper bound established until now for deterministic finite sets χ is due to Xia [18] who proves that the stretch factor is lower than 1.998. For the lower bound, Xia and Zhang [19] find a configuration of points χ such that the stretch factor is greater than 1.5932 (e.g. Figure 1 provides a configuration where the stretch factor is close to $\pi/2 \simeq 1.5708$).

In this paper, we focus on a probabilistic version of the problem by taking a slight modification of the underlying point process. More precisely, we consider a homogeneous Poisson point process X_n of intensity n in all the plane \mathbb{R}^2 . For such an infinite point process, studying the maximum of the stretch over any points $s, t \in X_n$ has no real sense. Indeed, for any bounded set $B \subset \mathbb{R}^2$, there exists a configuration of points in $X_n \cap B$ close to the one depicted in Figure 1 with non-zero probability. In particular, such a configuration occurs almost surely somewhere in the plane.

Contributions The main focus of our paper is to provide bounds for the expectation of the stretch factor between two fixed points $s, t \in \mathbb{R}^2$ in the Delaunay triangulation $\text{Del}(X)$, where $X := X_n \cup \{s, t\}$. The difficulty to obtain a lower bound for $\mathbb{E}[\ell(SP_X)]$ comes from the fact that we absolutely do not know where the shortest path SP_X is. We take the challenge by establishing our first main theorem.

Theorem 1. *Let $X := X_n \cup \{s, t\}$, where X_n is a Poisson point process of intensity n and $s, t \in \mathbb{R}^2$. Then*

$$\mathbb{P}[\ell(SP_X) \leq (1 + 2.47 \cdot 10^{-11})\|s - t\|] = O\left(n^{-\frac{1}{2}}\right).$$

As a consequence, we easily deduce the following result:

Corollary 2. *Let $X := X_n \cup \{s, t\}$, where X_n is a Poisson point process of intensity n and $s, t \in \mathbb{R}^2$. Then*

$$\liminf_{n \rightarrow \infty} \mathbb{E}\left[\frac{\ell(SP_X)}{\|s - t\|}\right] \geq 1 + 2.47 \cdot 10^{-11}.$$

We think that our results provide the first non-trivial lower bound (i.e. greater than 1) for the stretch factor when the intensity of the underlying Poisson point process goes to infinity. However, our lower bound is far from optimal since simulations suggest that $\lim_{n \rightarrow \infty} \mathbb{E}\left[\frac{\ell(SP_X)}{\|s - t\|}\right] \simeq 1.04$. We notice that our result is closely related to a theorem recently proved by Hirsch, Neuhaüser, and Schmidt [15, Theorem 26]. Indeed, they show that $\inf_{n \geq 1} \mathbb{E}\left[\frac{\ell(SP_X)}{\|s - t\|}\right] > 1$. However, their technique cannot provide explicit lower bound for the stretch factor. In the following proposition, we also give an upper bound.

Theorem 3. *Let $X := X_n \cup \{s, t\}$, where X_n is a Poisson point process of intensity n and $s, t \in \mathbb{R}^2$. Then*

$$\limsup_{n \rightarrow \infty} \mathbb{E}\left[\frac{\ell(SP_X)}{\|s - t\|}\right] \leq \frac{35}{3\pi^2} \simeq 1.182.$$

The upper bound we considered above is established by bounding the length of a particular path in the Delaunay triangulation. In particular, our theorem improves a result due to Baccelli et al. [2]. Indeed, by considering another particular path, they prove that the expectation of the stretch factor is lower than $\frac{4}{\pi} \simeq 1.27$.

Outline In Section 2, we begin with some preliminaries by introducing notation and tools of stochastic and integral geometry. As a first result, we use these tools in the next section to obtain a tight evaluation of the size of the straight walk. In particular, this evaluation gives an explicit value for the constant appearing in the work by Bose and Devroye [3] which was hidden in the asymptotic complexities. In Section 4, we provide estimates for the length of a particular path. These estimates directly imply Theorem 3. Section 5 constitutes the main part of our paper and deals with the lower bound for the shortest path. Our main idea is to discretize the plane into pixels and to consider the so-called lattice animals. We derive Theorem 1 by investigating the size of these lattice animals and by adapting tools of percolation theory. In Section 6, we give experimental values for various quantities. These simulations confirm the results for the size and the length of the straight walk and suggest that the correct value of the expected stretch factor is 1.04. In Appendix, we give auxiliary results which are used throughout the paper.

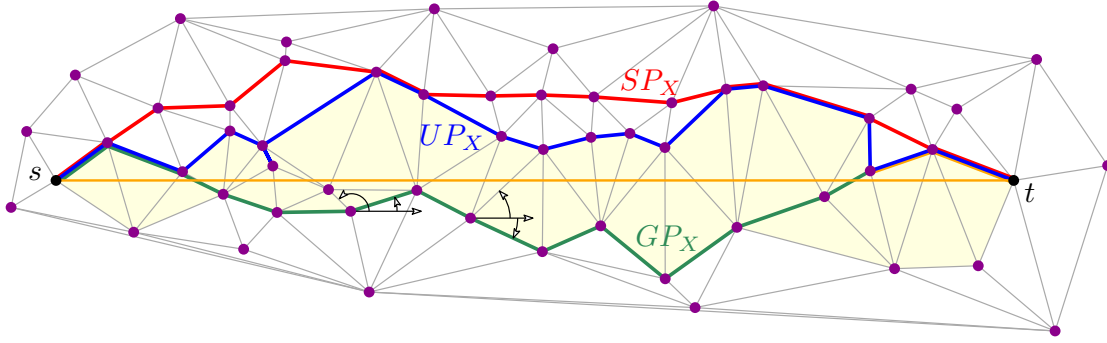


Figure 2: The paths SP_X , UP_X , and GP_X (the path GP_X is defined in Section 6).

2 Preliminaries

Notation Let s and t be two fixed points in \mathbb{R}^2 . Let X_n be a homogenous Poisson point process of intensity n in \mathbb{R}^2 and $X := X_n \cup \{s, t\}$. We denote by $\text{Del}(X)$ the Delaunay triangulation associated with X . We give below several notation which will be used throughout the paper.

- For any point $p \in \mathbb{R}^2$, we write $p = (x_p, y_p)$.
- For any segment $e \subset \mathbb{R}^2$, we denote by $h(e)$ and $|\hat{e}|$ the length of the horizontal projection of e and the absolute value of the angle with the x -axis respectively.
- For any k -tuple of points $p_1, \dots, p_k \in \mathbb{R}^2$, we write $p_{1:k} := (p_1, \dots, p_k)$. When $p_1, \dots, p_k \in \mathbb{R}^2$ are pairwise distinct, we write the k -tuple of points as $p_{1 \neq k}$. Such a notation will be used in the summation index. Moreover, with a slight abuse of notation, we write $\{p_{1:k}\} := \{p_1, \dots, p_k\}$.
- For each 3-tuple of points $p_{1 \neq 3} \in (\mathbb{R}^2)^3$ which do not belong to the same line, we denote by $\Delta(p_{1:3})$ and $B(p_{1:3})$ the triangle spanned by $p_{1:3}$ and the (open) circumdisk associated with $p_{1:3}$ respectively. We also denote by $R(p_{1:3})$ the radius of $B(p_{1:3})$.
- For each $z \in \mathbb{R}^2$ and $r \geq 0$, let $B(z, r)$ be the disk centered at z with radius r .
- Let $\mathbb{S} \subset \mathbb{R}^2$ be the unit circle endowed with its uniform distribution σ such that $\sigma(\mathbb{S}) = 2\pi$.
- For any Borel subset $B \subset \mathbb{R}^2$, let $\mathcal{A}(B)$ be the area of B . In particular, for each $u_{1:3} \in \mathbb{S}^3$, we have

$$\mathcal{A}(\Delta(u_{1:3})) = \frac{1}{2} \left| \det \begin{pmatrix} 1 & 1 & 1 \\ \cos \beta_1 & \cos \beta_2 & \cos \beta_3 \\ \sin \beta_1 & \sin \beta_2 & \sin \beta_3 \end{pmatrix} \right|,$$

where $\beta_i \in [0, 2\pi)$ is the angle between u_i and $(1, 0)$, with $1 \leq i \leq 3$.

Paths Given $s, t \in \mathbb{R}^2$, we denote by $\mathcal{P}_{s,t}(X)$ the family of paths in $\text{Del}(X)$ starting from s and going to t , with $X := X_n \cup \{s, t\}$. For each path $P \in \mathcal{P}_{s,t}(X)$, we denote by $\ell(P)$ the Euclidean length of P and $\text{Card}(P)$ its number of edges. We introduce two types of paths in $\mathcal{P}_{s,t}(X)$, namely SP_X and UP_X as follows:

Shortest Path SP_X : this path is the one which minimizes the length between s and t in the Delaunay triangulation $\text{Del}(X)$.

Upper Path UP_X : this path is defined as the set of all edges in $\mathbb{R} \times \mathbb{R}_+$ which belong to Delaunay triangles that intersects $[s, t]$. Some of these edges may be traversed in both ways (e.g. this is the case for the edges incident to the fifth vertex of the blue path in Figure 2).

These two paths are depicted in Figure 2 and described below. A third path, referred to as the greedy path GP_X , is also depicted in Figure 2 but introduced in Section 6.

Slivnyak-Mecke and Blaschke-Petkantschin Formulas Throughout the paper, we will extensively use two classical formulas of stochastic and integral geometry. As a warm-up, we first provide a new proof of a well-known result (usually established with the Euler relation) to introduce the computation technique with an easy pedagogical case.

Proposition 4. *Let X_n be a Poisson point process of intensity n and let N_0 be the number of triangles in $\text{Del}(X_n)$ whose circumdisk contains the origin. Then $\mathbb{E}[N_0] = 4$.*

Proof. First we notice that

$$\mathbb{E}[N_0] = \frac{1}{3!} \mathbb{E} \left[\sum_{\substack{p_{1:3} \in X_n^3 \\ p_1 \neq p_2 \neq p_3}} \mathbb{1}_{[\Delta(p_{1:3}) \in \text{Del}(X_n)]} \mathbb{1}_{[O \in B(p_{1:3})]} \right].$$

A first tool allows us to re-write the right-hand side as an integral. More precisely, according to the Slivnyak-Mecke formula (e.g. [17, Theorem 3.3.5]), we have

$$\begin{aligned} \mathbb{E}[N_0] &= \frac{n^3}{3!} \int_{(\mathbb{R}^2)^3} \mathbb{P}[\Delta(p_{1:3}) \in \text{Del}(X_n \cup \{p_{1:3}\})] \mathbb{1}_{[O \in B(p_{1:3})]} dp_{1:3} \\ &= \frac{n^3}{6} \int_{(\mathbb{R}^2)^3} e^{-n \mathcal{A}(B(p_{1:3}))} \mathbb{1}_{[O \in B(p_{1:3})]} dp_{1:3} \end{aligned}$$

since X_n is a Poisson point process. A second formula transforms the integral over $(\mathbb{R}^2)^3$ as an integral over $\mathbb{R}^2 \times \mathbb{R}_+ \times \mathbb{S}^3$ by associating with each $p_{1:3} \in (\mathbb{R}^2)^3$ the circumcenter, the circumradius and the angles of p_i , $1 \leq i \leq 3$, respectively. More precisely, from the Blaschke-Petkantschin formula (e.g. [17, Theorem 7.3.1]), we have

$$\mathbb{E}[N_0] = \frac{n^3}{6} \int_{\mathbb{R}_+} \int_{\mathbb{R}^2} \int_{\mathbb{S}^3} e^{-n \mathcal{A}(B(z,r))} \mathbb{1}_{[O \in B(z,r)]} \cdot r^3 2 \mathcal{A}(\Delta(u_{1:3})) \sigma(du_{1:3}) dz dr.$$

Integrating over z by noting that $O \in B(z, r) \iff z \in B(O, r)$, we get

$$\mathbb{E}[N_0] = \frac{\pi n^3}{6} \int_{\mathbb{R}_+} e^{-n\pi r^2} r^5 dr \times \int_{\mathbb{S}^3} 2 \mathcal{A}(\Delta(u_{1:3})) \sigma(du_{1:3})$$

since $\int_{B(O,r)} dz = \pi r^2$ for each $r \geq 0$. It follows that

$$\begin{aligned} \mathbb{E}[N_0] &= \frac{\pi n^3}{6} \int_{\mathbb{R}_+} e^{-n\pi r^2} r^5 dr \times \int_{[0,2\pi]^3} \left| \det \begin{pmatrix} 1 & 1 & 1 \\ \cos \beta_1 & \cos \beta_2 & \cos \beta_3 \\ \sin \beta_1 & \sin \beta_2 & \sin \beta_3 \end{pmatrix} \right| d\beta_{1:3} \\ &= \frac{\pi n^3}{6} \times \frac{1}{\pi^3 n^3} \times 24\pi^2 = 4. \end{aligned}$$

□

As written above, we add slanted red boxes in equations to give some explanation of the computation which often appear in the paper. A table of integrals is provided in Appendix B.

As a second easy warm up, we deal with the sum of the lengths of the Delaunay edges with respect to a typical vertex. In the following proposition, we only give an upper-bound for such a length since it is enough for us in the sequel.

Proposition 5. *Let X_n be a Poisson point process of intensity n and let L_0 be the sum of the lengths of the edges with vertex O in $\text{Del}(X_n \cup \{O\})$, where $O \in \mathbb{R}^2$ denotes the origin. Then $\mathbb{E}[L_0] = c \cdot n^{-\frac{1}{2}}$ for some constant c .*

In the above proposition, we do not make explicit the constant c . However, experimental values suggest that $c \simeq 6.8$.

Proof. The sum of the length of the edges L_0 can be expressed as

$$\mathbb{E}[L_0] = \frac{1}{2} \mathbb{E} \left[\sum_{p_1 \neq p_2 \in X_n^2} \mathbb{1}_{[\Delta(p_1 p_2 O) \in \text{Del}(X_n \cup \{O\})]} (\|p_1\| + \|p_2\|) \right].$$

The first factor $\frac{1}{2}$ comes from the fact that each triangle is counted twice (once clockwise and once counterclockwise). The second factor $\frac{1}{2}$ results from the fact that each edge is also obtained twice (once for each incident triangle). It follows that

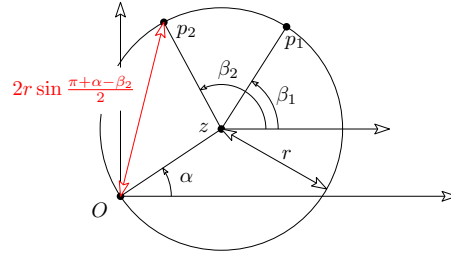
$$\mathbb{E}[L_0] = \frac{n^2}{4} \int_{(\mathbb{R}^2)^2} \mathbb{P}[\Delta(p_1 p_2 O) \in \text{Del}(X_n \cup \{p_1, p_2, O\})] (\|p_1\| + \|p_2\|) dp_1 dp_2. \quad (1)$$

To make explicit the right-hand side, we give an analogous version of the Blaschke- Petkanschin type change of variables in which one of the vertices is held fixed. We proceed in the same spirit as in Schneider and Weil [17, proof of Theorem 7.3.2]. More precisely, let ϕ be the function

$$\begin{aligned} \phi : \mathbb{R}_+ \times [0, 2\pi)^3 &\longrightarrow \mathbb{R}^2 \times \mathbb{R}^2 \\ (r, \alpha, \beta_1, \beta_2) &\longmapsto (p_1, p_2), \end{aligned}$$

where, for each $i = 1, 2$, we let

$$p_i = r(\cos \alpha + \cos \beta_i, \sin \alpha + \sin \beta_i).$$



Provided that O , p_1 and p_2 do not belong to the same line, we notice that r and $z := r(\cos \alpha, \sin \alpha)$ are the circumradius and the circumcenter of the triangle $\Delta(O, p_1, p_2)$ respectively. The terms β_1 and β_2 represent the angles of the vectors $\overrightarrow{z p_1}$ and $\overrightarrow{z p_2}$ with respect to the x -axis. Up to a null set, the function ϕ defines a C^1 diffeomorphism with Jacobian $J_\phi(r, \alpha, \beta_1, \beta_2) := r^3 \cdot D(\alpha, \beta_1, \beta_2)$, where

$$D(\alpha, \beta_1, \beta_2) := \begin{vmatrix} \cos \alpha + \cos \beta_1 & -\sin \alpha & -\sin \beta_1 & 0 \\ \sin \alpha + \sin \beta_1 & \cos \alpha & \cos \beta_1 & 0 \\ \cos \alpha + \cos \beta_2 & -\sin \alpha & 0 & -\sin \beta_2 \\ \sin \alpha + \sin \beta_2 & \cos \alpha & 0 & \cos \beta_2 \end{vmatrix}$$

Since $\|p_i\| = 2r \left| \cos \frac{\beta_i - \alpha}{2} \right|$ with $(p_1, p_2) = \phi(r, \alpha, \beta_1, \beta_2)$, it follows from (1) that

$$\begin{aligned} \mathbb{E}[L_0] &= \frac{n^2}{4} \int_{\mathbb{R}_+} \int_{[0, 2\pi]^3} e^{-n\pi r^2} 2r \left(\left| \cos \frac{\beta_1 - \alpha}{2} \right| + \left| \cos \frac{\beta_2 - \alpha}{2} \right| \right) \\ &\quad \times r^3 \cdot |D(\alpha, \beta_1, \beta_2)| d\alpha d\beta_1 d\beta_2 dr \\ &= \frac{n^2}{4} \cdot \frac{3}{8\pi^2 n^2 \sqrt{n}} \stackrel{\text{Eq. (13)}}{=} 2 \int_{[0, 2\pi]^3} \left(\left| \cos \frac{\beta_1 - \alpha}{2} \right| + \left| \cos \frac{\beta_2 - \alpha}{2} \right| \right) |D(\alpha, \beta_1, \beta_2)| d\alpha d\beta_1 d\beta_2 dr \end{aligned}$$

It follows that $\mathbb{E}[L_0] = c \cdot n^{-\frac{1}{2}}$ since the integral over $[0, 2\pi]^3$ is finite. \square

3 Size of Straight Walk

In this section and in the next one, we restrict our interest to triangles which are cut by the line segment $[s, t]$. We first investigate the mean number of edges for the straight walk.

Proposition 6. *Let $X := X_n \cup \{s, t\}$, where X_n is a Poisson point process of intensity n and $s, t \in \mathbb{R}^2$. Let $N_{s,t}$ be the number of edges of triangles in $\text{Del}(X)$ intersecting $[s, t]$. Then*

$$\mathbb{E} \left[\frac{N_{s,t}}{\|s-t\|} \right] = \frac{64}{3\pi^2} \sqrt{n} + O(1) \simeq 2.1615 \sqrt{n}.$$

Even if the previous proposition is not closely related to the shortest path, we think that our result could help us for a better understanding of SP_X . In particular, the tools appearing in the proof of Proposition 6 will be useful in the following sections.

Proof. Without loss of generality, we assume that $s = (0, 0)$ and $t = (1, 0)$. First we notice that almost surely

$$N_{s,t} = \frac{1}{2} \sum_{p_{1:3} \in X_n^3} \mathbb{1}_{[\Delta(p_{1:3}) \in \text{Del}(X)]} \mathbb{1}_{[p_{1:3} \in E^+]} + \frac{1}{2} \sum_{p_{1:3} \in X_n^3} \mathbb{1}_{[\Delta(p_{1:3}) \in \text{Del}(X)]} \mathbb{1}_{[p_{1:3} \in E^-]} + 1, \quad (2)$$

where

$$\begin{aligned} E^+ &:= \{p_{1:3} \in (\mathbb{R}^2)^3 : \Delta(p_{1:3}) \cap [s, t] \neq \emptyset, B(p_{1:3}) \cap \{s, t\} = \emptyset, y_{p_1}, y_{p_2} > 0, y_{p_3} < 0\}, \\ E^- &:= \{p_{1:3} \in (\mathbb{R}^2)^3 : \Delta(p_{1:3}) \cap [s, t] \neq \emptyset, B(p_{1:3}) \cap \{s, t\} = \emptyset, y_{p_1}, y_{p_2} < 0, y_{p_3} > 0\}. \end{aligned}$$

In the same spirit as above, we also define a third set which will be useful in the sequel as

$$E'^+ := \{p_{1:3} \in (\mathbb{R}^2)^3 : \Delta(p_{1:3}) \cap \text{line}(s, t) \neq \emptyset, y_{p_1}, y_{p_2} > 0, y_{p_3} < 0\}.$$

Notice that the factor $\frac{1}{2}$ appearing in (2) comes from the fact that each triangle of E is obtained twice, with counterclockwise and clockwise orientations. Indeed, the triangles crossed by $[s, t]$ have vertices in X_n except the first and the last ones which are incident to s and t respectively. Besides, the number of edges crossed by $[s, t]$ is one less than the number of triangles intersecting $[s, t]$, which explains the term $+1$ in Equation (2).

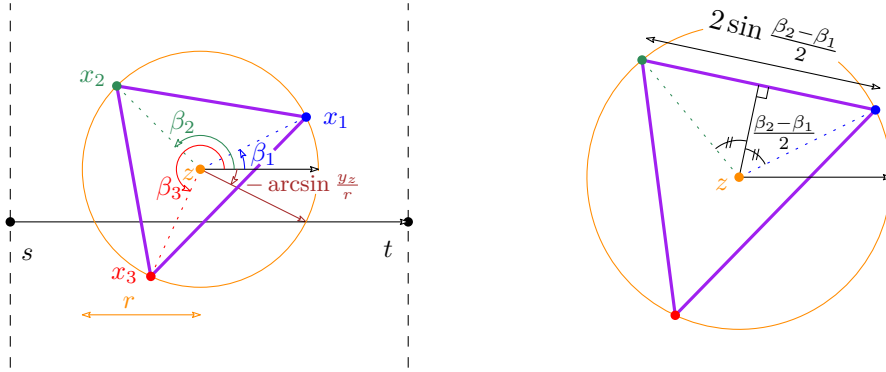


Figure 3: Notation for the proofs of Propositions 6 and 7.

Provided that $p_{1:3} \in E^+$, we notice that $\Delta(p_{1:3})$ is a triangle in $\text{Del}(X)$ if and only if it is a triangle in $\text{Del}(X_n)$. This implies that

$$\mathbb{E} \left[\sum_{p_{1 \neq 3} \in X_n^3} \mathbb{1}_{[\Delta(p_{1:3}) \in \text{Del}(X)]} \mathbb{1}_{[p_{1:3} \in E^+]} \right] = \mathbb{E} \left[\sum_{p_{1 \neq 3} \in X_n^3} \mathbb{1}_{[\Delta(p_{1:3}) \in \text{Del}(X_n)]} \mathbb{1}_{[p_{1:3} \in E^+]} \right].$$

Besides, thanks to the Slivnyak-Mecke formula, we have

$$\mathbb{E} \left[\sum_{p_{1 \neq 3} \in X_n^3} \mathbb{1}_{[\Delta(p_{1:3}) \in \text{Del}(X_n)]} \mathbb{1}_{[p_{1:3} \in E^+]} \right] = n^3 \int_{(\mathbb{R}^2)^3} \mathbb{P}[X \cap B(p_{1:3}) = \emptyset] \mathbb{1}_{[p_{1:3} \in E^+]} dp_{1:3}.$$

When $p_{1:3} \in E^+$, the circumdisk $B(p_{1:3})$ intersects $[s, t]$ and does not contain s or t . In particular, we have $z(p_{1:3}) \in [0, 1] \times [-R(p_{1:3}), R(p_{1:3})]$. It follows from the Blaschke-Petkantschin formula that

$$\begin{aligned} & \mathbb{E} \left[\sum_{p_{1 \neq 3} \in X_n^3} \mathbb{1}_{[\Delta(p_{1:3}) \in \text{Del}(X_n)]} \mathbb{1}_{[p_{1:3} \in E^+]} \right] \\ &= n^3 \int_0^\infty \int_0^1 \int_{-r}^r \int_{\mathbb{S}^3} e^{-n\pi r^2} \mathbb{1}_{[z+ru_{1:3} \in E^+]} \cdot r^3 2 \mathcal{A}(\Delta(u_{1:3})) \sigma(du_{1:3}) dy_z dx_z dr. \end{aligned} \quad (3)$$

Let $r > 0$ be fixed. First, we make explicit the integral over y_z and $u_{1:3}$ in the above equation when we replace the set E^+ by E'^+ . By taking the change of variables $h = \frac{y_z}{r}$ (see Figure 3), we have

$$\begin{aligned} & \int_{-r}^r \int_{\mathbb{S}^3} 2 \mathcal{A}(\Delta(u_{1:3})) \mathbb{1}_{[z+ru_{1:3} \in E'^+]} \sigma(du_{1:3}) dy_z \\ &= r \int_{-1}^1 \int_{\pi+\arcsin h}^{2\pi-\arcsin h} \int_{-\arcsin h}^{\pi+\arcsin h} \int_{-\arcsin h}^{\pi+\arcsin h} \left| \det \begin{pmatrix} 1 & 1 & 1 \\ \cos \beta_1 & \cos \beta_2 & \cos \beta_3 \\ \sin \beta_1 & \sin \beta_2 & \sin \beta_3 \end{pmatrix} \right| d\beta_1 d\beta_2 d\beta_3 dh = \frac{512}{9} r. \end{aligned}$$

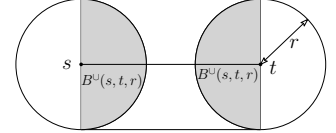
Eq. (21)

We can evaluate the right-hand side of Equation (3) by substituting E^+ by E'^+ as follows:

$$\begin{aligned} n^3 \int_0^\infty \int_0^1 \int_{-r}^r \int_{\mathbb{S}^3} e^{-n\pi r^2} \mathbb{1}_{[z+ru_{1:3} \in E'^+]} \cdot r^3 2 \mathcal{A}(\Delta(u_{1:3})) \sigma(du_{1:3}) dy_z dx_z dr \\ = \frac{512n^3}{9} \int_0^\infty \int_0^1 e^{-n\pi r^2} r^4 dx_z dr = \frac{512n^3}{9} \cdot \frac{3}{8\pi^2 n^2 \sqrt{n}} \stackrel{\text{Eq. (13)}}{=} \frac{64}{3\pi^2} \sqrt{n}. \end{aligned} \quad (4)$$

To prove that the right-hand side of (3) has the same order when we replace E^+ by E'^+ , we define:

$$B^\cup(s, t, r) := (B(s, r) \cap \{z; x_z \geq 0\}) \cup (B(t, r) \cap \{z; x_z \leq 1\}).$$



When $z + ru_{1:3} \in E'^+$ and $z \in ([0, 1] \times [-r, r]) \setminus B^\cup(s, t, r)$, we have $z + ru_{1:3} \in E^+$. This implies that

$$0 \leq (\mathbb{1}_{[z+ru_{1:3} \in E'^+]} - \mathbb{1}_{[z+ru_{1:3} \in E^+]}) \mathbb{1}_{[z \in [0, 1] \times [-r, r]]} \leq \mathbb{1}_{[z \in B^\cup(s, t, r)]}$$

Moreover, we have

$$n^3 \int_0^\infty \int_{B^\cup(s, t, r)} \int_{\mathbb{S}^3} e^{-n\pi r^2} \cdot r^3 2 \mathcal{A}(\Delta(u_{1:3})) \sigma(du_{1:3}) dz dr = 24. \quad \text{as in Prop. 4}$$

This together with (3) and (4) shows that

$$\frac{64}{3\pi^2} \sqrt{n} - 24 \leq \mathbb{E} \left[\sum_{p_1 \neq 3} \mathbb{1}_{[\Delta(p_{1:3}) \in \text{Del}(X_n)]} \mathbb{1}_{[p_{1:3} \in E^+]} \right] \leq \frac{64}{3\pi^2} \sqrt{n}.$$

Proceeding along the same lines as above, we obtain exactly the same bounds when we replace E^+ by E^- . This proves Proposition 6 by plugging this value in Equation (2) since

$$\frac{64}{3\pi^2} \sqrt{n} - 23 \leq \mathbb{E} \left[\frac{N_{s,t}}{\|s - t\|} \right] \leq \frac{64}{3\pi^2} \sqrt{n} + 1.$$

□

4 Length of the Upper Path

In this section, we estimate the expectation and the variance of the length of the upper path UP_X . The following proposition deals with the expectation.

Proposition 7. *Let X_n be a Poisson point process of intensity n and $X := X_n \cup \{s, t\}$ with $s, t \in \mathbb{R}^2$. Let $\ell(UP_X)$ be the length of the upper path UP_X in $\text{Del}(X)$ from s to t . Then*

$$\mathbb{E} \left[\frac{\ell(UP_X)}{\|s - t\|} \right] = \frac{35}{3\pi^2} + O\left(n^{-\frac{1}{2}}\right) \simeq 1.182.$$

The above result provides an upper bound for the expectation of the length of the shortest path and implies directly Theorem 3.

Proof. The proof is closely related to the one of Proposition 6. Indeed, assuming without loss of generality that $s = (0, 0)$ and $t = (1, 0)$, we define

$$L_{X_n} := \sum_{p_1 \neq_{1,3} \in X_n^3} l_{X_n}(p_{1:3}), \quad (5)$$

with

$$l_{X_n}(p_{1:3}) = \frac{1}{2} \mathbb{1}_{[\Delta(p_{1:3}) \in \text{Del}(X_n)]} \mathbb{1}_{[p_{1:3} \in E^+]} \|p_2 - p_1\|.$$

In the expression of L_{X_n} , we have considered the lengths of the edges in UP_X , excepted the ones which contain the points s and t . By Proposition 5, the expected lengths of these two edges is $O\left(n^{-\frac{1}{2}}\right)$. Hence, it is enough to show that $\mathbb{E}[L_{X_n}] = \frac{35}{3\pi^2} + O\left(n^{-\frac{1}{2}}\right)$. To do it, we apply the Slivnyak-Mecke and the Blaschke-Petkantschin formulas. This gives

$$\mathbb{E}[L_{X_n}] = \frac{1}{2} n^3 \int_{\mathbb{R}_+} \int_{\mathbb{R}^2} \int_{\mathbb{S}^3} e^{-n\pi r^2} \mathbb{1}_{[z+ru_{1:3} \in E^+]} r \|u_2 - u_1\| r^3 2 \mathcal{A}(\Delta(u_{1:3})) \sigma(du_{1:3}) dy_z dx_z dr, \quad (6)$$

where we recall that $z = (x_z, y_z)$. In the same spirit as Proposition 6, we have:

$$0 \leq \left(\mathbb{1}_{[z+ru_{1:3} \in E'^+]} - \mathbb{1}_{[z+ru_{1:3} \in E^+]} \right) \mathbb{1}_{[z \in [0,1] \times [-r,r]]} \|u_2 - u_1\| \leq 2 \cdot \mathbb{1}_{[z \in B^\cup(s,t,r)]}$$

and

$$\begin{aligned} & n^3 \int_0^\infty \int_{B^\cup(s,t,r)} \int_{\mathbb{S}^3} e^{-n\pi r^2} r^4 2 \mathcal{A}(\Delta(u_{1:3})) \sigma(du_{1:3}) dy_z dx_z dr \\ & \leq n^3 \int_0^\infty \frac{\mathcal{A}(B^\cup(s,t,r))}{\pi r^2} \int_{\mathbb{S}^3} e^{-n\pi r^2} r^4 2 \mathcal{A}(\Delta(u_{1:3})) \sigma(du_{1:3}) dy_z dx_z dr \\ & \leq \pi n^3 \times \frac{15}{16\pi^3 n^{\frac{7}{2}}} \times 24\pi^2 = \frac{45}{2\sqrt{n}} = 22.5 n^{-\frac{1}{2}}. \end{aligned}$$

Replacing E^+ by E'^+ in (6), it follows that:

$$\mathbb{E}[L_{X_n}] = \frac{n^3}{2} \int_0^\infty \int_0^1 \int_{-r}^r \int_{\mathbb{S}^3} e^{-n\pi r^2} \mathbb{1}_{[z+ru_{1:3} \in E'^+]} \|u_2 - u_1\| r^4 2 \mathcal{A}(\Delta(u_{1:3})) \sigma(du_{1:3}) dy_z dx_z dr + O\left(n^{-\frac{1}{2}}\right).$$

Let $r \geq 0$ be fixed. By taking the change of variables $h = \frac{yz}{r}$ (see Figure 3), we obtain

$$\begin{aligned} & \int_{-r}^r \int_{\mathbb{S}^3} \mathbb{1}_{[z+ru_{1:3} \in E'+]} \|u_2 - u_1\| \mathcal{A}(\Delta(u_{1:3})) \sigma(du_{1:3}) dy_z \\ &= r \int_{-1}^1 \int_{\pi+\arcsin h}^{2\pi-\arcsin h} \int_{-\arcsin h}^{\pi+\arcsin h} \int_{-\arcsin h}^{\beta_2} \det \begin{pmatrix} 1 & 1 & 1 \\ \cos \beta_1 & \cos \beta_2 & \cos \beta_3 \\ \sin \beta_1 & \sin \beta_2 & \sin \beta_3 \end{pmatrix} \\ & \quad \times 2 \sin \frac{\beta_2 - \beta_1}{2} d\beta_1 d\beta_2 d\beta_3 dh \\ &= \frac{35\pi}{3} r. \end{aligned} \tag{Eq. (22)}$$

It follows that

$$\mathbb{E}[L_{X_n}] = n^3 \cdot \frac{35\pi}{3} \int_0^\infty \int_0^1 e^{-n\pi r^2} r^5 dx_z dr + O\left(n^{-\frac{1}{2}}\right) = \frac{35}{3\pi^2} + O\left(n^{-\frac{1}{2}}\right). \tag{Eq. (14)}$$

□

The following proposition deals with the variance of the length of the upper path.

Proposition 8. *Let X_n be a Poisson point process of intensity n and $X := X_n \cup \{s, t\}$ with $s, t \in \mathbb{R}^2$. Let $\ell(UP_X)$ be the length of the upper path UP_X in $\text{Del}(X)$ from s to t . Then*

$$\mathbb{V}\left[\frac{\ell(UP_X)}{\|s - t\|}\right] = O\left(n^{-\frac{1}{2}}\right).$$

The proof uses similar tools as the one for the expected value and is postponed to Appendix A. As a corollary, we obtain an estimate of the tail of the length of the upper path.

Corollary 9. *With the same notation as above, we have*

$$\mathbb{P}[\ell(UP_X) > 1.2\|s - t\|] = O\left(n^{-\frac{1}{2}}\right).$$

Proof. It follows from the Chebyshev's inequality that

$$\mathbb{P}[\ell(UP_X) > 1.2\|s - t\|] \leq \frac{\mathbb{V}[\ell(UP_X)]}{1.2\|s - t\| - \mathbb{E}[\ell(UP_X)]}.$$

This concludes the proof according to Proposition 7 and Proposition 8. □

5 Lower Bound on Shortest Path

In this section, we prove Theorem 1. By scaling invariance, our problem is the same as if the intensity n is constant and $s = (0, 0)$, $t = (k, 0)$, where $k \in \mathbb{N}^*$ goes to infinity.

Before starting our proof, we give the main ideas. First, we discretize the plane \mathbb{R}^2 into squares $C(v)$, which will be called pixels, with $v \in \mathbb{Z}^2$. The set of pixels intersecting the smallest path SP_X will be called the lattice animal associated with SP_X . In a sense which will be specified, we associate with each pixel $C(v)$ a (strong) horizontality property which ensures that there exists a path "almost horizontal" in the Delaunay triangulation through the pixel $C(v)$. Then, we proceed into four steps.

1. We begin with preliminaries by introducing formally the notions of animal lattice and strong horizontality property.
2. We give an upper bound for the size of the associated lattice animal (Corollary 12). Moreover, given a property \mathcal{Y} , we provide an upper bound for the probability that the number of pixels in the lattice animal with property \mathcal{Y} is large. This result will be applied to the case where \mathcal{Y} is the horizontality property (Proposition 13).
3. We establish a lower bound for the length of any path with respect to the number of pixels with a strong horizontality property in the associated lattice animal (Lemma 14).
4. We prove that the probability that a pixel has a (strong) horizontality property is small (Proposition 15).
5. We conclude our proof by combining the steps described above (Section 5.5).

5.1 Preliminaries

5.1.1 Animal lattices

Recall that $s = (0, 0)$ and $t = (k, 0)$ for some integer k . We discretize \mathbb{R}^2 into pixels as follows. Let $\mathbf{G} = (\mathbb{Z}^2, E)$ be the graph with set of edges satisfying $(v, w) \in E \Leftrightarrow \|v - w\| = 1$, where $v, w \in \mathbb{Z}^2$. In digital geometry, the graph is known as a *4-connected neighborhood* and each vertex of \mathbf{G} is called a *pixel*. Moreover, for each $v \in \mathbb{Z}^2$, we consider different scaled versions of squares (see: Figure 4-left)

$$C(v) := v \oplus [-\frac{1}{2}, \frac{1}{2}]^2, \quad C^\varepsilon(v) := v \oplus [-\frac{1}{2} - \varepsilon, \frac{1}{2} + \varepsilon]^2; \quad C_\lambda(v) := v \oplus [-\frac{\lambda}{2}, \frac{\lambda}{2}]^2,$$

where \oplus denotes the Minkowski sum, $\lambda \in \mathbb{Z}$ and $\varepsilon \in \mathbb{R}_+^*$. With a slight abuse of notation, we also say that $C(v)$ is a pixel.

We define scaled and translated versions of the grid \mathbf{G} as follows. For $\lambda \in \mathbb{Z}$ and $\tau \in \mathbb{Z}^2$ we denote by $\lambda\mathbf{G}$ the grid of points in $(\lambda\mathbb{Z})^2$ with edges of length λ and $\tau + \lambda\mathbf{G}$ its translation by τ . We also split \mathbf{G} in 4 subgrids as follows: each subgrid is referred to as a color $c \in \text{Colors}$, where $\text{Colors} := \{\text{green}, \text{pink}, \text{blue}, \text{yellow}\}$. Each subgrid with color c is denoted:

$$\mathbf{G}_c = 2\mathbf{G} + O_c,$$

where

$$O_{(\text{green})} = (0, 0), \quad O_{(\text{pink})} = (1, 0), \quad O_{(\text{blue})} = (0, 1), \quad \text{and} \quad O_{(\text{yellow})} = (1, 1).$$

Notice that when v and w are two pixels with the same color, the squares $C_2(v)$ and $C_2(w)$ have disjoint interior. Such a property will be useful to ensure the independence of a suitable family of random variables.

We conclude this section with the so-called notion of animal [9]. Given a graph $G' := (V', E')$, a *lattice animal* is a collection of vertices $\mathbf{A} \subset V'$ such that for every pair of distinct vertices $v, w \in \mathbf{A}$ there is a path in G' connecting v, w visiting only vertices in \mathbf{A} . With each path P in the Delaunay triangulation, we associate the so-called lattice animal of P in \mathbf{G} (see Figure 5):

$$\mathbf{A}(P) = \{v \text{ vertex of } \mathbf{G} : C(v) \cap P \neq \emptyset\}.$$

In the same spirit as above, for each $c \in \text{Colors}$, we let

$$\mathbf{A}_{(c)}(P) = \{v \text{ vertex of } \mathbf{G}_{(c)} : C_2(v) \cap P \neq \emptyset\}$$

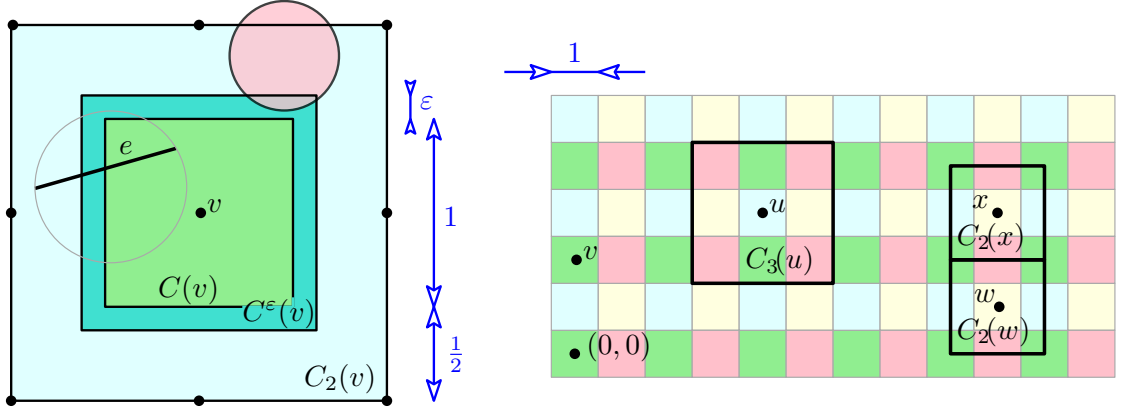
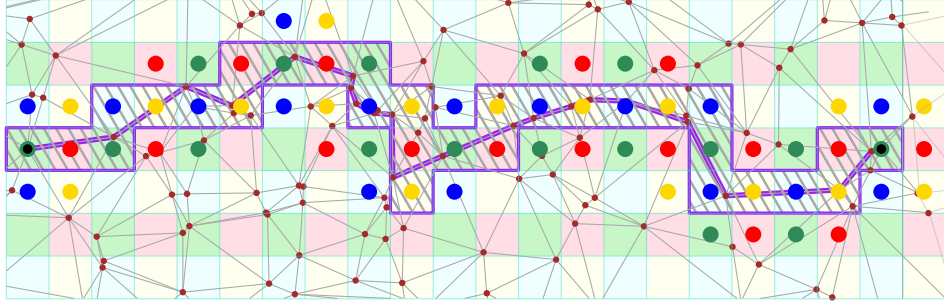


Figure 4: Squares definitions.

Figure 5: Lattice animals. The pixels $C(v)$ for $v \in \mathbf{A}(P)$ are hashed and the path P is purple. The $\mathbf{A}_{(c)}(P)$, for each $c \in \text{Colors}$, are referred to as big dots of the relevant color.

We also considered animals at different scales (see Figure 7):

$$\mathbf{A}_{(c),\lambda}(P) = \{v \text{ vertex of } \lambda\mathbf{G} + O_c : C_\lambda(v) \cap P \neq \emptyset\}.$$

5.1.2 Properties on pixels

For any pixel $v \in \mathbb{Z}^2$, we consider three events, namely $\mathcal{I}_\varepsilon(v)$, $\mathcal{H}_\rho(v)$, and $\mathcal{H}'_{\varepsilon,\alpha,\kappa}(v)$. These events depend on four parameters $\varepsilon > 0$, $\rho > 0$, $\alpha \in [0, \frac{\pi}{2}]$, and $\kappa > 1$ and are described below.

- *Independence property* $\mathcal{I}_\varepsilon(v)$: this event holds if, for any Delaunay triangle in $\text{Del}(X)$ intersecting $C^\varepsilon(v)$, the circumdisk of the triangle is included in $C_2(v)$ and $\|s - v\| \geq 2$ and $\|t - v\| \geq 2$ (to avoid pixels that are neighbors of s or t). Notice that this event is $\sigma(X_n \cap C_2(v))$ measurable.
- *Strong horizontality property* $\mathcal{H}_\rho(v)$: this event holds if there exists a path along Delaunay edges in $\text{Del}(X)$, between $x_v - \frac{1}{2}$ and $x_v + \frac{1}{2}$, intersecting $C(v)$ and with length smaller than $1 + \rho$. A path satisfying this property is denoted by $\mathcal{PH}_\rho(v)$. Besides, the first and the last edges of such a path are clipped by the vertical lines $x = x_v - \frac{1}{2}$ and $x = x_v + \frac{1}{2}$.

- *Weak horizontality property* $\mathcal{H}'_{\varepsilon,\alpha,\kappa}(v)$: this event holds if the total length $L_{\varepsilon,\alpha,\kappa}(v)$ of the horizontal projection of all edges in $\text{Del}(X)$ intersecting $C^\varepsilon(v)$ and having an angle with respect to the x -axis smaller than α , is greater than $\frac{1}{\kappa}$, i.e.

$$L_{\varepsilon,\alpha,\kappa}(v) = \sum_{e, e \cap C^\varepsilon(v) \neq \emptyset, |\widehat{e}| \leq \alpha} h(e) \geq \frac{1}{\kappa}.$$

5.2 Animals

5.2.1 Size of animals

We establish below a series of results on the size of animals obtained from a discretization of some path starting from s and going to t with $s, t \in \mathbb{Z}^2$. The following lemma is due to Gerard, Favreau and Vacavant [14]. For completeness, we give a more concise proof of their result.

Lemma 10. *Let $s, t \in \mathbb{R}^2$ and let P be a path between s and t (not necessarily in $\text{Del } X$). Then*

$$\text{Card}(\mathbf{A}(P)) \leq \frac{3\sqrt{2}}{2}\ell(P) + 1 \simeq 2.12\ell(P) + 1.$$

Proof. Let $P := \{e_1, \dots, e_k\}$ be a path between s and t , with $e_i := [Z_{i-1}, Z_i]$ for each $1 \leq i \leq k$ and $Z_0 = s$ and $Z_k = t$. We can construct an auxiliary path P'' with the same lattice animal as P and such that $\ell(P'') \leq \ell(P)$ by straightening the path P between the intersections of P and the boundaries of pixels $C(v)$, $v \in \mathbb{Z}^2$ (see Figure 6-left). Then, we can construct a path P' from P'' , again with the same lattice animal as P , with $\ell(P') \leq \ell(P'')$, and such that the vertices of P' belong to the set of corners of pixels. The path P' is defined by moving the vertices of P'' along the boundaries of pixels in the direction that shorten the path, up to a corner or up to the point that aligns the two incident segments. In particular, the new path is such that $\mathbf{A}(P) = \mathbf{A}(P')$ and $\ell(P) \geq \ell(P')$. Hence, without loss of generality, we can assume that $Z_i \in (\frac{1}{2}, \frac{1}{2}) + \mathbb{Z}^2$ for each $1 \leq i \leq k-1$.

Denoting by $E_i := \bigcup_{j=0}^i e_j$, we trivially obtain that

$$\text{Card}(\mathbf{A}(P)) = \sum_{i=1}^k \text{Card}(\mathbf{A}'(e_i)),$$

where

$$\mathbf{A}'(e_i) = \{v \in \mathbb{Z}^2 : C(v) \cap e_i \neq \emptyset \text{ and } C(v) \cap E_{i-1} = \emptyset\}.$$

We provide below an upper bound for $\text{Card}(\mathbf{A}'(e_i))$. Indeed, for each edge $e_i := [Z_{i-1}, Z_i]$, $2 \leq i \leq k-1$, we consider the rectangle $[x_{Z_{i-1}}, x_{Z_i}] \times [y_{Z_{i-1}}, y_{Z_i}]$ (see Figure 6-center). If $x_{Z_{i-1}} = x_{Z_i}$ or $y_{Z_{i-1}} = y_{Z_i}$, we trivially obtain that $\text{Card}(\mathbf{A}'(e_i)) \leq 2 \cdot \ell(e_i)$. If not, we notice that $\text{Card}(\mathbf{A}'(e_i)) = a_i + b_i + 1$ and $\ell(e_i) = \sqrt{a_i^2 + b_i^2}$ with $a_i = |x_{Z_{i-1}} - x_{Z_i}|$ and $b_i = |y_{Z_{i-1}} - y_{Z_i}|$. Besides, we can easily prove that for each $a, b > 0$, we have $\frac{a+b+1}{\sqrt{a^2+b^2}} \leq \frac{3\sqrt{2}}{2}$ (the equality holds when $a = b = 1$). This implies that $\text{Card}(\mathbf{A}'(e_i)) \leq \frac{3\sqrt{2}}{2} \cdot \ell(e_i)$. Finally we have $\ell(e_1) = \ell(e_k) = \frac{\sqrt{2}}{2}$, $\text{Card}(\mathbf{A}'(e_1)) = 4$, and $\text{Card}(\mathbf{A}'(e_k)) = 0$. It follows that

$$\text{Card}(\mathbf{A}(P)) \leq 4 + \sum_{i=2}^{k-1} \frac{3\sqrt{2}}{2} \cdot \ell(e_i) = \frac{3\sqrt{2}}{2} \cdot \ell(P) + 1.$$

In Figure 6-right, we depict a path P such that $\text{Card}(\mathbf{A}(P)) \simeq \frac{3\sqrt{2}}{2}\ell(P) + 1 \simeq 2.12\ell(P) + 1$, which shows that our upper bound in Lemma 10 is tight. \square

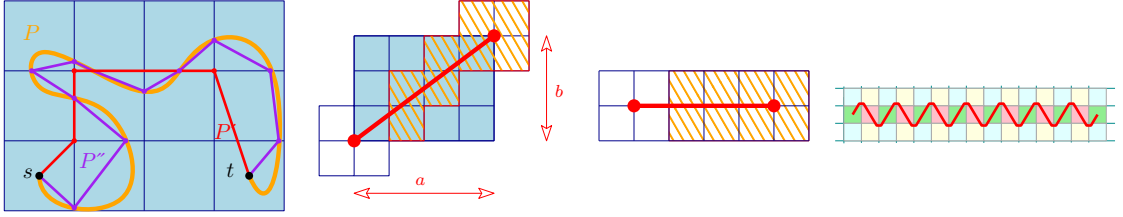


Figure 6: Illustration for the proof of Lemma 10. Left: A realization of the paths P , P'' , and P' . Center: hatched pixels are charged to the red edge. Right: The red path visits 3 pixels per column and has a length close to $\sqrt{2}$ per column (2 pixels in the first and last column with length $\frac{\sqrt{2}}{2}$ in these columns).

As a corollary, we obtain a deterministic upper bound for the size of the animal associated with the shortest path.

Corollary 11. *Let $SP_X \in \mathcal{P}_{s,t}(X)$ with $\|s - t\| = k$. Then*

$$\text{Card}(\mathbf{A}(SP_X)) < 4.24k + 1 \quad \text{and} \quad \forall \lambda \in \mathbb{Z}, \text{Card}(\mathbf{A}_{(c),\lambda}(SP_X)) < \frac{4.24k}{\lambda} + 1.$$

Proof. The first result is a direct consequence of Lemma 10 and the fact that $\ell(SP_X) < 1.998k$ according to the main result of Xia [18]. The second one is obtained by applying the first result to the grid $\lambda\mathbf{G}$. \square

The following result provides a better upper bound for the size of the animal with high probability.

Corollary 12. *Let $SP_X \in \mathcal{P}_{s,t}(X)$ with $\|s - t\| = k$. For any $\lambda > 0$, $c \in \text{Colors}$, and $k > 0$, let $\mathcal{E}(c, k, \lambda)$ be the event:*

$$\mathcal{E}(c, k, \lambda) := \left\{ \text{Card}(\mathbf{A}_{(c),\lambda}(SP_X)) < \frac{2.55k}{\lambda} + 1 \right\}. \quad (7)$$

Then $\mathbb{P}[\mathcal{E}(c, k, \lambda)] = 1 - O\left(k^{-\frac{1}{2}}\right)$.

Proof. This is a probabilistic version of Corollary 11 obtained by bounding the length of SP_X by the one of UP_X instead of using the deterministic bound due to Xia. Corollary 9 ensures that the upper bound for the length of UP_X holds with probability $1 - O\left(k^{-\frac{1}{2}}\right)$. The constant comes from the fact that $1.2 \cdot 2.12 < 2.55$. \square

5.2.2 Animal lemma

In this section, we establish a result which ensures that the number of pixels in $\mathbf{A}(SP_X)$ which satisfy a property \mathcal{Y} is not large with high probability. In the sequel, we will use the following notation:

$$\mathbb{Z}_{s,t}^2 := \mathbb{Z}^2 \setminus \{v \in \mathbb{Z}^2 : \|v - s\| \leq 2 \text{ or } \|v - t\| \leq 2\}.$$

For each color c , we also let $\mathbb{Z}_{s,t}^{2,(c)} := \mathbb{Z}_{s,t}^2 \cap \{v \in \mathbb{Z}^2 \text{ with color } c\}$.

Proposition 13. *Let $p \in (0, 0.01]$ and let $\mathcal{Y} := (Y_v)_{v \in \mathbb{Z}^2}$ be a family of events such that, for any color c , the events $(Y_v)_{v \in \mathbb{Z}_{s,t}^{2,(c)}}$ are independent and $p = \mathbb{P}[Y_v]$ for each $v \in \mathbb{Z}_{s,t}^{2,(c)}$. For any $\mathbf{A} \subset \mathbb{Z}^2$, we denote by $\#\mathcal{Y}(\mathbf{A}) = \sum_{v \in \mathbf{A}} \mathbb{1}_{[Y_v]}$ the number of pixels v in \mathbf{A} such that the event Y_v holds. Then, we have*

$$\mathbb{P}[\#\mathcal{Y}(\mathbf{A}_{(c)}(SP_X)) \geq 4k\sqrt{p}] = O(k^{-\frac{1}{2}}).$$

Proof. Our proof relies on an adaptation of a result due to Devillers and Hemsley [10, Lemma 7]. The main idea is to discretize the shortest path at different scales and to use standard ideas of (site) percolation theory. Let $\lambda \in 4\mathbb{Z} + 2$. This restriction on λ ensures that $\forall v \in \mathbf{G}_c, \forall w \in \lambda\mathbf{G} + O_c : C_2(v) \cap C_\lambda(w) \neq \emptyset \Rightarrow C_2(v) \subset C_\lambda(w)$. Taking $\mathcal{E}(c, k, \lambda)$ as in (7), we obtain for each $x > 0$, that

$$\begin{aligned} \mathbb{P}[\#\mathcal{Y}(\mathbf{A}_{(c)}(SP_X)) \geq xk\sqrt{p}] &= \mathbb{P}[\{\#\mathcal{Y}(\mathbf{A}_{(c)}(SP_X)) \geq xk\sqrt{p}\} \cap \mathcal{E}(c, k, \lambda)] \\ &\quad + \mathbb{P}[\{\#\mathcal{Y}(\mathbf{A}_{(c)}(SP_X)) \geq xk\sqrt{p}\} \cap (\neg\mathcal{E}(c, k, \lambda))]. \end{aligned}$$

From Corollary 12, it follows that

$$\mathbb{P}[\#\mathcal{Y}(\mathbf{A}_{(c)}(SP_X)) \geq xk\sqrt{p}] \leq \mathbb{P}[\{\#\mathcal{Y}(\mathbf{A}_{(c)}(SP_X)) \geq xk\sqrt{p}\} \cap \mathcal{E}(c, k, \lambda)] + O(k^{-\frac{1}{2}}).$$

The animal $\mathbf{A}_{(c),\lambda}(SP_X)$ can be viewed as a sequence of connected squares of size λ , starting at the square containing s . Besides, on the event $\mathcal{E}(c, k, \lambda)$, the animal $\mathbf{A}_{(c),\lambda}(SP_X)$ belongs to the family $\mathcal{A}_{(c),\lambda}(k)$ of animals $\mathbf{A} \subset \lambda\mathbf{G} + O_c$ such that $O_c \in \mathbf{A}$ and $\text{Card}(\mathbf{A}) \leq \lfloor \frac{2.55k}{\lambda} + 1 \rfloor$. Each animal $\mathbf{A} \in \mathcal{A}_{(c),\lambda}(k)$ can be encoded as a word on four letters $\{S, E, N, W\}$ (standing for south, east, north, and west) of length $\text{Card}(\mathbf{A})$. Hence, $\text{Card}(\mathcal{A}_{(c),\lambda}(k)) \leq 4^{\lfloor \frac{2.55k}{\lambda} + 1 \rfloor} \leq 4^{\frac{2.55k}{\lambda} + 1}$. Moreover, since $\lambda \in 4\mathbb{Z} + 2$, we have

$$\mathbf{A}_{(c)}(SP_X) \subset \mathbf{A}_{(c),\lambda}^{(\lambda)}(SP_X),$$

where, for all animal $\mathbf{A} \subset \lambda\mathbf{G} + O_c$, we let $\mathbf{A}^{(\lambda)} := \{v \in \mathbf{G}_{(c)} : \exists w \in \mathbf{A}, v \in C_\lambda(w)\}$ (see Figure 7). This implies that for each $x > 0$, we have

$$\begin{aligned} \mathbb{P}[\{\#\mathcal{Y}(\mathbf{A}_{(c)}(SP_X)) \geq xk\sqrt{p}\} \cap \mathcal{E}(c, k, \lambda)] &\leq \mathbb{P}[\{\#\mathcal{Y}(\mathbf{A}_{(c),\lambda}^{(\lambda)}(SP_X)) \geq xk\sqrt{p}\} \cap \mathcal{E}(c, k, \lambda)] \\ &\leq \mathbb{P}\left[\bigcup_{\mathbf{A} \in \mathcal{A}_{(c),\lambda}(k)} \{\#\mathcal{Y}(\mathbf{A}^{(\lambda)}) \geq xk\sqrt{p}\}\right] \\ &\leq \sum_{\mathbf{A} \in \mathcal{A}_{(c),\lambda}(k)} \mathbb{P}[\#\mathcal{Y}(\mathbf{A}^{(\lambda)}) \geq xk\sqrt{p}] \tag{8} \\ &\leq \sum_{\mathbf{A} \in \mathcal{A}_{(c),\lambda}(k)} \mathbb{P}\left[\sum_{v \in \mathbf{A}^{(\lambda)} \cap \mathbb{Z}_{s,t}^{2,(c)}} \mathbb{1}_{[Y_v]} \geq xk\sqrt{p} - 10\right]. \end{aligned}$$

The last inequality comes from the fact that $\sum_{v \in \mathbf{A}^{(\lambda)} \cap \mathbb{Z}_{s,t}^{2,(c)}} \mathbb{1}_{[Y_v]} \geq \#\mathcal{Y}(\mathbf{A}^{(\lambda)}) - 10$ since the number of pixels in \mathbb{Z}^2 with color c , which are not in $\mathbb{Z}_{s,t}^{2,(c)}$, is lower than 10. From the assumption of

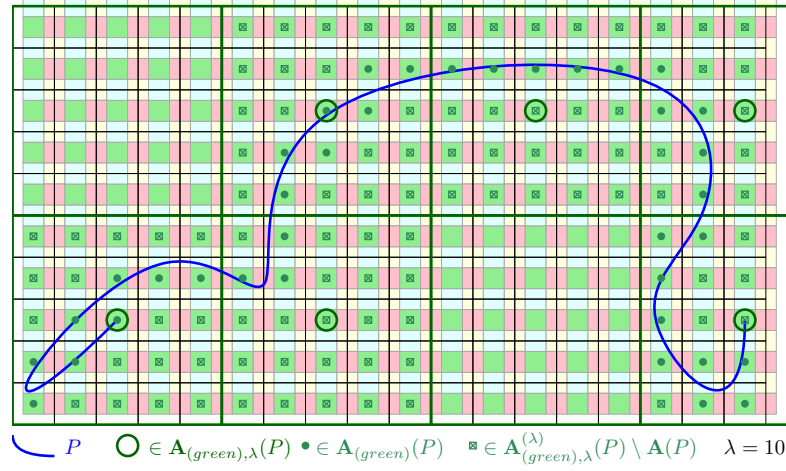


Figure 7: The set $\mathbf{A}^{(\lambda)}_{(green),\lambda}(P)$ for a path P .

Proposition 13, we know that for each $\mathbf{A} \in \mathcal{A}_{(c),\lambda}(k)$, the random variable $\sum_{v \in \mathbf{A}^{(\lambda)} \cap \mathbb{Z}_{s,t}^{2,(c)}} \mathbb{1}_{[Y_v]}$ is a binomial distribution with parameters (N, p) , where $N := \text{Card}(\mathbf{A}^{(\lambda)} \cap \mathbb{Z}_{s,t}^{2,(c)}) \leq 0.64\lambda k$ since $\text{Card}(\mathbf{A}^{(\lambda)}) \leq \frac{2.55k}{\lambda} \frac{\lambda^2}{4} + 1$, $s \in \mathbf{A}^{(\lambda)} \setminus \mathbb{Z}_{s,t}^{2,(c)}$, and $\frac{2.55}{4} \leq 0.64$.

According to the Chernoff's inequality, we obtain for all $\mathbf{A} \in \mathcal{A}_{(c),\lambda}(k)$ that

$$\begin{aligned} \mathbb{P} \left[\sum_{v \in \mathbf{A}^{(\lambda)} \cap \mathbb{Z}_{s,t}^{2,(c)}} \mathbb{1}_{[Y_v]} \geq xk\sqrt{p} - 10 \right] &\leq e^{-xk\sqrt{p}+10} \cdot \mathbb{E} \left[e^{\sum_{v \in \mathbf{A}^{(\lambda)} \cap \mathbb{Z}_{s,t}^{2,(c)}} \mathbb{1}_{[Y_v]}} \right] \\ &= e^{-xk\sqrt{p}+10} \cdot ((1-p) + pe)^{\text{Card}(\mathbf{A}^{(\lambda)} \cap \mathbb{Z}_{s,t}^{2,(c)})} \\ &\leq e^{-xk\sqrt{p}+10} \cdot (1 + p(e-1))^{0.64\lambda k}. \end{aligned}$$

This together with (8) and the fact that $\text{Card}(\mathcal{A}_{(c),\lambda}(k)) \leq 4^{\frac{2.55k}{\lambda}+1}$ implies that

$$\mathbb{P} [\{\#\mathcal{Y}(\mathbf{A}_{(c)}(SP_X)) \geq xk\sqrt{p}\} \cap \mathcal{E}(c, k, \lambda)] \leq 4^{\frac{2.55k}{\lambda}+1} \cdot e^{-xk\sqrt{p}+10} \cdot (1 + p(e-1))^{0.64\lambda k}.$$

With standard computations, we get

$$\begin{aligned} \mathbb{P} [\{\#\mathcal{Y}(\mathbf{A}_{(c)}(SP_X)) \geq xk\sqrt{p}\} \cap \mathcal{E}(c, k, \lambda)] &\leq 4^{\frac{2.55k}{\lambda}+1} \cdot e^{-xk\sqrt{p}+10} \cdot (1 + p(e-1))^{0.64\lambda k} \\ &\leq 4^{\frac{2.55k}{\lambda}+1} \cdot e^{-xk\sqrt{p}+10} \cdot (e^{p(e-1)})^{0.64\lambda k} \\ &= 4e^{10} \cdot \exp \left(\log 4 \cdot \frac{2.55k}{\lambda} - xk\sqrt{p} + 0.64 p(e-1)\lambda k \right) \\ &\leq 4e^{10} \cdot \exp \left(-k\sqrt{p} \left(x - \left(\frac{3.54}{\lambda\sqrt{p}} + 1.1\lambda\sqrt{p} \right) \right) \right) \\ &\leq 4e^{10} e^{-(x-3.98)k\sqrt{p}} \quad \text{by choosing } \lambda \in \left[\frac{1.6}{\sqrt{p}}, \frac{2}{\sqrt{p}} \right] \cap (4\mathbb{Z} + 2) \\ &= o(k^{-\frac{1}{2}}) \quad \text{by choosing } x = 4 \text{ for any fixed } p \text{ when } k \rightarrow \infty. \end{aligned}$$

The fact that a suitable $\lambda \in \left[\frac{1.6}{\sqrt{p}}, \frac{2}{\sqrt{p}}\right] \cap (4\mathbb{Z} + 2)$ exists is ensured by the condition $p < 0.01$. \square

5.3 A lower bound for the length of a path

We establish below a lower bound for the length of any path with respect to the number of pixels with a strong horizontality property.

Lemma 14. *Let $P \in \mathcal{P}_{s,t}(X)$ and $\rho > 0$. Then*

$$\ell(P) \geq k + \rho \left(k - 4 \max_{c \in \text{Colors}} \#\mathcal{H}(\mathbf{A}_{(c)}(P)) \right),$$

where $\#\mathcal{H}(\mathbf{A}_{(c)}(P))$ is the number of pixels v in $\mathbf{A}_{(c)}(P)$ such that $\mathcal{H}_\rho(v) \vee \neg \mathcal{I}_{\varepsilon_\rho}(v)$.

Proof. Splitting the path P into vertical columns, we have $\ell(P) = \sum_{i \in \mathbb{Z}} \ell(P \cap \text{Col}[i])$, where, for each $i \in \mathbb{Z}$, $\text{Col}[i] = [i - \frac{1}{2}, i + \frac{1}{2}] \times \mathbb{R}$ is the i th column. For $i \in \{1, \dots, k-1\}$, let $v[i]$ be the lowest pixel of $\mathbf{A}(P) \cap \text{Col}[i]$ such that there is a connected component of $P \cap \text{Col}[i]$ intersecting $C(v[i])$ and the left and right side of $\text{Col}[i]$. Notice that such a pixel exists for each column $1 \leq i \leq k-1$. On the event $\neg \mathcal{H}_\rho(v[i]) \wedge \mathcal{I}_{\varepsilon_\rho}(v[i])$, we use the fact that $\ell(P \cap \text{Col}[i]) \geq 1 + \rho$. On the complement of this event, we use the trivial inequality $\ell(P \cap \text{Col}[i]) \geq 1$. Denoting by $N := \sum_{i=1}^{k-1} \mathbb{1}_{[\mathcal{H}_\rho(v[i]) \vee \neg \mathcal{I}_{\varepsilon_\rho}(v[i])]}$ the number of horizontal pixels on the path, it follows that

$$\begin{aligned} \ell(P) &\geq \sum_{i=1}^{k-1} \mathbb{1}_{[\mathcal{H}_\rho(v[i]) \vee \neg \mathcal{I}_{\varepsilon_\rho}(v[i])]} + \sum_{i=1}^{k-1} (1 + \rho) \mathbb{1}_{[\neg \mathcal{H}_\rho(v[i]) \wedge \mathcal{I}_{\varepsilon_\rho}(v[i])]} \\ &\geq N + (1 + \rho)(k - N) = k + \rho(k - N). \end{aligned}$$

Then we conclude the proof by observing that

$$N \leq \sum_{v \in \mathbf{A}(P)} \mathbb{1}_{[\mathcal{H}_\rho(v) \vee \neg \mathcal{I}_{\varepsilon_\rho}(v)]} \leq \sum_{c \in \text{Colors}} \#\mathcal{H}(\mathbf{A}_{(c)}(P)) \leq 4 \max_{c \in \text{Colors}} \#\mathcal{H}(\mathbf{A}_{(c)}(P)).$$

\square

5.4 Probability that a pixel has a strong horizontality property

To apply Proposition 13, we have to estimate the probability of the event $\mathcal{H}_\rho(v) \vee \neg \mathcal{I}_{\varepsilon_\rho}(v)$. An upper bound for this probability is given in the following result.

Proposition 15. *Let $v \in \mathbb{Z}_{s,t}^2$ and $0 < \rho < 4 \cdot 10^{-6}$ and let $\varepsilon_\rho := \sqrt{\rho} \sqrt{2 + \rho}$. Then*

$$\mathbb{P}[\mathcal{H}_\rho(v) \vee \neg \mathcal{I}_{\varepsilon_\rho}(v)] \leq P(\rho, n),$$

where

$$P(\rho, n) := 95n^3 e^{-0.194n} + (19n^2 + 13n + 4) e^{-n\pi} + 31.76 \left(\frac{3}{4} + \frac{\sqrt{\rho} \sqrt{\rho + 2}}{2} \right)^2 \sqrt{\rho n}.$$

One of the main difficulties to prove Theorem 1 is actually contained in the above result. To pave the way, we proceed into two steps. First, we choose parameters ε and α in such a way that the strong horizontality property is stronger than the weak horizontality property. Secondly, we provide bounds for the probability that a pixel has a weak horizontality property or an independence property.

5.4.1 Strong vs weak horizontality

Lemma 16. *Let $v \in \mathbb{Z}^2$ and $\rho > 0$ and let $\varepsilon_\rho := \sqrt{\rho}\sqrt{2+\rho}$. If the property $\mathcal{H}_\rho(v)$ holds, then $\mathcal{PH}_\rho(v) \subset C^{\varepsilon_\rho}(v)$.*

Proof. Assume that $v = 0$ without loss of generality. Up to a vertical translation, the shortest path between the lines $x = -\frac{1}{2}$ and $x = \frac{1}{2}$ crossing $C(0)$ and intersecting the complement of $C^{\varepsilon_\rho}(0)$ is the segment from $(-\frac{1}{2}, \frac{1}{2})$ to $(\frac{1}{2}, \frac{1}{2} + \varepsilon_\rho)$. Since the length of this segment is $\sqrt{1 + \varepsilon_\rho^2} = 1 + \rho$, we necessarily have $\mathcal{PH}_\rho(v) \subset C^{\varepsilon_\rho}(v)$. \square

Lemma 17. *Let $v \in \mathbb{Z}^2$ and $\rho > 0$ and $0 < \kappa < 1$ such that $\frac{\kappa}{\kappa-1}\rho < \frac{\pi^2}{8}$ and let $\alpha_{\rho,\kappa} := \sqrt{2\frac{\kappa}{\kappa-1}\rho}$. If the property $\mathcal{H}_\rho(v)$ holds then the same is true for $\mathcal{H}'_{\varepsilon_\rho, \alpha_{\rho,\kappa}, \kappa}(v)$.*

Proof. We make a proof by contradiction, assuming $\mathcal{H}_\rho(v)$ and $\neg\mathcal{H}'_{\varepsilon_\rho, \alpha_{\rho,\kappa}, \kappa}(v)$. The main idea is to split the edges e in $\mathcal{PH}_\rho(v)$ with respect to their angles $|\widehat{e}|$. Indeed,

$$1 + \rho \geq \ell(\mathcal{PH}_\rho(v)) = \sum_{e \in \mathcal{PH}_\rho(v), |\widehat{e}| \leq \alpha_{\rho,\kappa}} \ell(e) + \sum_{e \in \mathcal{PH}_\rho(v), |\widehat{e}| > \alpha_{\rho,\kappa}} \ell(e),$$

where the inequality comes from the property $\mathcal{H}_\rho(v)$. For each $e \in \mathcal{PH}_\rho(v)$, we use the trivial inequality $l(e) \geq h(e)$ when $|\widehat{e}| \leq \alpha_{\rho,\kappa}$. If $|\widehat{e}| > \alpha_{\rho,\kappa}$, we notice that, for $\frac{\kappa}{\kappa-1}\rho < \frac{\pi^2}{8}$,

$$l(e) > \frac{h(e)}{\cos \alpha_{\rho,\kappa}} \geq \left(1 + \frac{\alpha_{\rho,\kappa}^2}{2}\right) h(e) = \left(1 + \frac{\kappa}{\kappa-1}\rho\right) h(e),$$

where the second inequality comes from the fact that $\frac{1}{\cos \alpha} \geq \left(1 + \frac{\alpha^2}{2}\right)$ for any $\alpha \in [0, \frac{\pi}{2})$.

It follows that

$$\begin{aligned} 1 + \rho &> \left(1 + \frac{\kappa}{\kappa-1}\rho - \frac{\kappa}{\kappa-1}\rho\right) \sum_{e \in \mathcal{PH}_\rho(v), |\widehat{e}| \leq \alpha_{\rho,\kappa}} h(e) + \left(1 + \frac{\kappa}{\kappa-1}\rho\right) \sum_{e \in \mathcal{PH}_\rho(v), |\widehat{e}| > \alpha_{\rho,\kappa}} h(e) \\ &= \left(1 + \frac{\kappa}{\kappa-1}\rho\right) \sum_{e \in \mathcal{PH}_\rho(v)} h(e) - \frac{\kappa}{\kappa-1}\rho \sum_{e \in \mathcal{PH}_\rho(v), |\widehat{e}| \leq \alpha_{\rho,\kappa}} h(e). \end{aligned}$$

By assumption, the property $\mathcal{H}'_{\varepsilon_\rho, \alpha_{\rho,\kappa}, \kappa}(v)$ does not hold. Then we deduce from Lemma 16 that

$$1 + \rho > \left(1 + \frac{\kappa}{\kappa-1}\rho\right) - \frac{\kappa}{\kappa-1}\rho L_{\varepsilon_\rho, \alpha_{\rho,\kappa}, \kappa}(v) > 1 + \frac{\kappa}{\kappa-1}\rho - \frac{\kappa}{\kappa-1}\rho \frac{1}{\kappa} = 1 + \rho,$$

getting a contradiction. \square

5.4.2 Pixel probabilities

Probability for the independence property First, we provide an upper bound for the probability that a pixel has the independence property.

Lemma 18. *Let $v \in \mathbb{Z}_{s,t}^2$ and let $\varepsilon < \frac{1}{700}$ be fixed. Then*

$$\mathbb{P}[\neg\mathcal{I}_\varepsilon(v)] \leq 95n^3 e^{-0.194n} + (19n^2 + 13n + 4) e^{-n\pi}.$$

In the above lemma, we have assumed that $\varepsilon < \frac{1}{700}$ to obtain an upper bound for $\mathbb{P}[\neg\mathcal{I}_\varepsilon(v)]$ which is independent of ε .

Proof. Let $N_\varepsilon(v)$ be the number of Delaunay triangles in $\text{Del}(X_n)$ such that the associated circumdisk intersects simultaneously $C^\varepsilon(v)$ and the complement of $C_2(v)$. If the event $\mathcal{I}_\varepsilon(v)$ does not hold, then $N_\varepsilon(v) \geq 1$ (here we have used the fact that $\mathcal{I}_\varepsilon(v)$ is $\sigma(X_n \cap C(v))$ measurable). It follows from the Markov's inequality that

$$\mathbb{P}[-\mathcal{I}_\varepsilon(v)] \leq \mathbb{P}[N_\varepsilon(v) \geq 1] \leq \mathbb{E}[N_\varepsilon(v)].$$

Besides,

$$\mathbb{E}[N_\varepsilon(v)] = \frac{1}{3!} \mathbb{E} \left[\sum_{p_{1,2,3} \in X_n^3} \mathbb{1}_{[\Delta(p_{1,2,3}) \in \text{Del}(X_n)]} \mathbb{1}_{[B(p_{1,2,3}) \not\subset C_2(v); B(p_{1,2,3}) \cap C^\varepsilon(v) \neq \emptyset]} \right].$$

It follows from the Slivnyak-Mecke and the Blaschke-Petkantschin formulas that

$$\begin{aligned} \mathbb{E}[N_\varepsilon(v)] &= \frac{n^3}{3!} \int_{(\mathbb{R}^2)^3} \mathbb{P}[B(z,r) \cap X_n = \emptyset] \mathbb{1}_{[B(z,r) \not\subset C_2(v); B(z,r) \cap C^\varepsilon(v) \neq \emptyset]} dp_{1,2,3} \\ &= \frac{n^3}{6} \int_{\mathbb{R}_+} \int_{\mathbb{R}^2} \int_{\mathbb{S}^3} e^{-n \mathcal{A}(B(z,r))} \mathbb{1}_{[B(z,r) \not\subset C_2(v); B(z,r) \cap C^\varepsilon(v) \neq \emptyset]} \\ &\quad \times r^3 2 \mathcal{A}(\Delta(u_{1,2,3})) \sigma(du_{1,2,3}) dz dr \\ &= \frac{n^3}{6} 24\pi^2 \int_{\mathbb{R}_+} \int_{\mathbb{R}^2} e^{-n\pi r^2} \mathbb{1}_{[B(z,r) \not\subset C_2(v); z \in C^\varepsilon(v) \oplus B(0,r)]} r^3 dz dr \end{aligned} \quad (9)$$

since $B(z,r) \cap C^\varepsilon(v) \neq \emptyset$ if and only if $z \in C^\varepsilon(v) \oplus B(0,r)$. To deal with $B(z,r) \not\subset C_2(v)$ we consider two cases as follows (see Figure 8):

Case 1: if $r \leq 1$, we use the fact that

$$\begin{cases} B(z,r) \not\subset C_2(v) \\ z \in C^\varepsilon(v) \oplus B(0,r) \end{cases} \Rightarrow z \in [-r - \frac{1}{2} - \varepsilon, r + \frac{1}{2} + \varepsilon]^2 \setminus [r-1, 1-r]^2.$$

Notice that we have to choose $r > \frac{1-2\varepsilon}{4} > 0.249$ to ensure that the set of the right-hand side is not empty. Besides, this set has an area smaller than $4(2r + \varepsilon - \frac{1}{2})(\frac{3}{2} + \varepsilon) < 12.016r$.

Case 2: if $r > 1$, we use the trivial assertion

$$\begin{cases} B(z,r) \not\subset C_2(v) \\ z \in C^\varepsilon(v) \oplus B(0,r) \end{cases} \Rightarrow z \in [-r - \frac{1}{2} - \varepsilon, r + \frac{1}{2} + \varepsilon]^2.$$

The set of the right-hand side has an area which is lower than $(1 + 2\varepsilon + 2r)^2 < 3.004r^2$. By integrating over z , it follows from (9) that

$$\begin{aligned} \mathbb{P}[-\mathcal{I}_\varepsilon(v)] &\leq 4\pi^2 n^3 \left(\int_{0.249}^1 e^{-n\pi r^2} 12.016 r^4 dr + \int_1^\infty e^{-n\pi r^2} 3.004 r^5 dr \right) \\ &\leq 4\pi^2 n^3 \left(e^{-n\pi 0.249^2} \int_{0.249}^1 12.016 r^4 dr + \int_1^\infty e^{-n\pi r^2} 3.004 r^5 dr \right) \\ &\leq 95n^3 e^{-0.194n} + (19n^2 + 13n + 4) e^{-n\pi}. \end{aligned} \quad \text{Eq (15)}$$

□

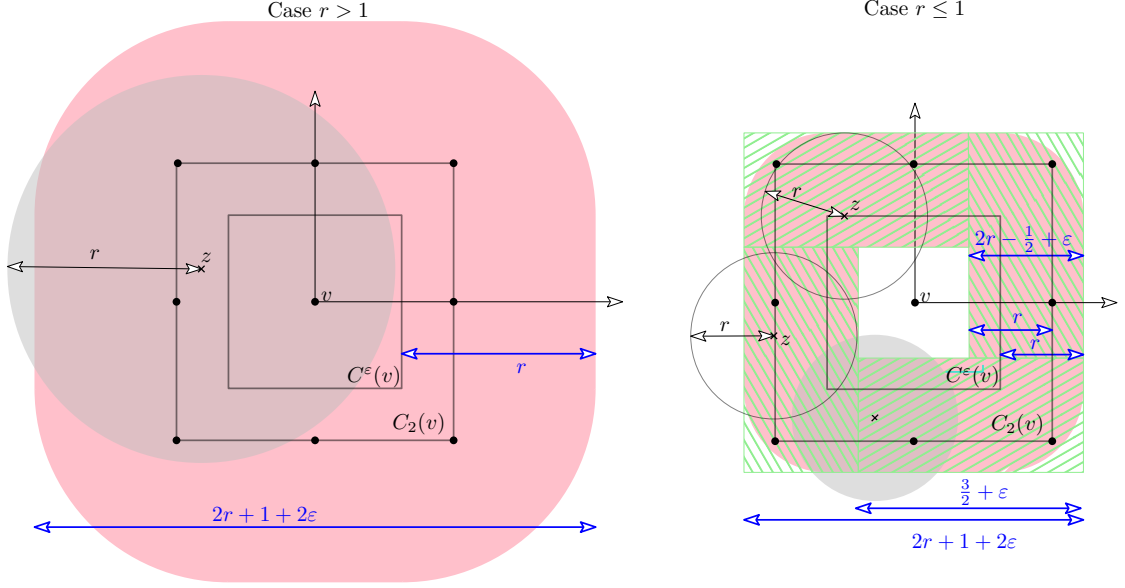


Figure 8: The squares $C^\varepsilon(v)$, $C_2(v)$ (black), the set $C^\varepsilon(v) \oplus B(0, r)$ (pink) and the disk $B(z, r)$ (grey).

Probability for the weak horizontality property Secondly, we provide an upper bound for the probability that a pixel has a weak horizontality property conditional on the fact that it has the independence property.

Lemma 19. *Let $v \in \mathbb{Z}_{s,t}^2$ and $\rho < 0.4$. Then there exists $\kappa > 0$ such that $\frac{\kappa}{\kappa-1}\rho < \frac{\pi^2}{8}$ and*

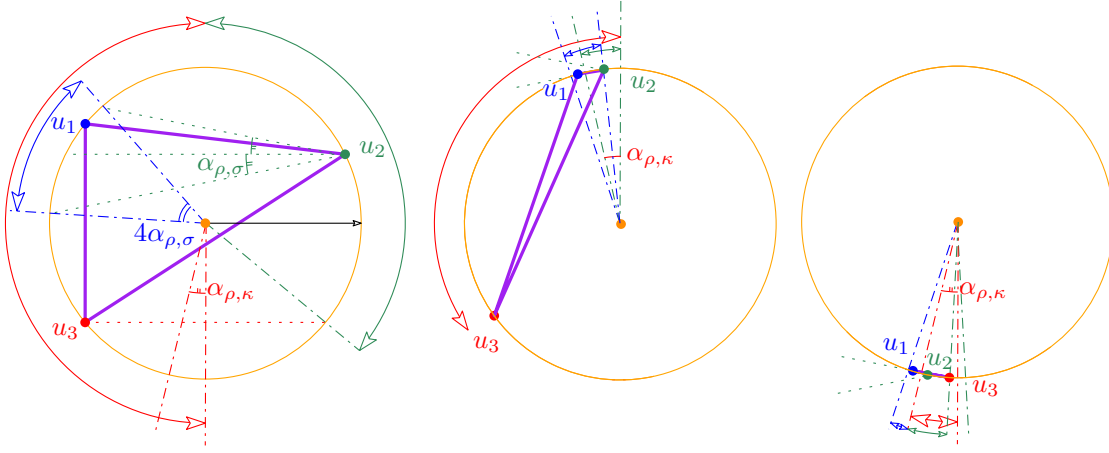
$$\mathbb{P}[\mathcal{I}_{\varepsilon_\rho}(v)] \mathbb{P}\left[\mathcal{H}'_{\varepsilon_\rho, \alpha_{\rho, \kappa}, \kappa}(v) \mid \mathcal{I}_{\varepsilon_\rho}(v)\right] \leq 31.8 \left(\frac{3}{4} + \frac{\sqrt{\rho}\sqrt{\rho+2}}{2}\right)^2 \sqrt{\rho n},$$

where $\varepsilon_\rho := \sqrt{\rho}\sqrt{2+\rho}$ and $\alpha_{\rho, \kappa} := \sqrt{2\frac{\kappa}{\kappa-1}\rho} \in [0, \frac{\pi}{2}]$ are the same as in Lemma 17.

Proof. According to the Markov's inequality, we have:

$$\begin{aligned} \mathbb{P}\left[\mathcal{H}'_{\varepsilon_\rho, \alpha_{\rho, \kappa}, \kappa}(v) \mid \mathcal{I}_{\varepsilon_\rho}(v)\right] &= \mathbb{P}\left[L_{\varepsilon_\rho, \alpha_{\rho, \kappa}, \kappa}(v) \geq \frac{1}{\kappa} \mid \mathcal{I}_{\varepsilon_\rho}(v)\right] \\ &\leq \kappa \mathbb{E}\left[L_{\varepsilon_\rho, \alpha_{\rho, \kappa}, \kappa}(v) \mid \mathcal{I}_{\varepsilon_\rho}(v)\right] \\ &= \frac{\kappa \mathbb{E}\left[L_{\varepsilon_\rho, \alpha_{\rho, \kappa}, \kappa}(v) \mathbb{1}_{[\mathcal{I}_{\varepsilon_\rho}(v)]}\right]}{\mathbb{P}[\mathcal{I}_{\varepsilon_\rho}(v)]}. \end{aligned} \quad (10)$$

Now, recalling that on the event $\mathcal{I}_{\varepsilon_\rho}(v)$, any triangle, and thus any edge, intersecting $C^{\varepsilon_\rho}(v)$

Figure 9: Domains of integration for $u(\beta_{1:3})$.

has its vertices inside $C_2(v)$, we have:

$$\begin{aligned} & \mathbb{E} \left[L_{\varepsilon, \alpha, \rho, \kappa}(v) \mathbb{1}_{[\mathcal{I}_{\varepsilon, \rho}(v)]} \right] \\ & \leq \frac{1}{2} \mathbb{E} \left[\sum_{\substack{p_{1:3} \in DT(X_n) \\ p_1 \neq p_2, p_3}} \mathbb{1}_{[|\widehat{p_1 p_2}| < \alpha_{\rho, \kappa}; x_{p_1} \leq x_{p_2}] \mathbb{1}_{[B(p_{1:3}) \subset C_2(v)]} \mathbb{1}_{[B(p_{1:3}) \cap C^{\varepsilon, \rho}(v) \neq \emptyset]} h(p_1 p_2) \right] \end{aligned}$$

where the $\frac{1}{2}$ factor comes from the fact that each edge is counted twice in the sum (once for each incident triangle). We apply the Slivnyak-Mecke and the Blaschke-Petkantschin formulas. This gives:

$$\begin{aligned} \mathbb{E} \left[L_{\varepsilon, \alpha, \rho, \kappa}(v) \mathbb{1}_{[\mathcal{I}_{\varepsilon, \rho}(v)]} \right] & \leq \frac{1}{2} n^3 \int_{C_2(v)} \int_0^1 \int_{\mathbb{S}^3} e^{-n \mathcal{A}(B(z, r))} \mathbb{1}_{[|\widehat{u_1 u_2}| < \alpha_{\rho, \kappa}; x_{u_1} \leq x_{u_2}] \\ & \quad \times \mathbb{1}_{[B(z, r) \subset C_2(v)]} \mathbb{1}_{[B(z, r) \cap C^{\varepsilon, \rho}(v) \neq \emptyset]} \cdot r h(u_1 u_2) \cdot r^3 2 \mathcal{A}(\Delta(u_{1:3})) \sigma(du_{1:3}) dr dz \end{aligned}$$

since $B(z, r) \subset C_2(v)$ implies that $z \in C_2(v)$ and $r \leq 1$. Hence, $\mathbb{E} \left[L_{\varepsilon, \alpha, \rho, \kappa}(v) \mathbb{1}_{[\mathcal{I}_{\varepsilon, \rho}(v)]} \right] \leq a(n, \rho) \times b(\rho, \kappa)$, where

$$\begin{aligned} a(n, \rho) & := \frac{1}{2} n^3 \int_{C_2(v)} \int_0^1 e^{-n \pi r^2} r^4 \mathbb{1}_{[B(z, r) \subset C_2(v)]} \mathbb{1}_{[B(z, r) \cap C^{\varepsilon, \rho}(v) \neq \emptyset]} dr dz. \\ b(\rho, \kappa) & := \int_{\mathbb{S}^3} \mathbb{1}_{[|\widehat{u_1 u_2}| < \alpha_{\rho, \kappa}; x_{u_1} \leq x_{u_2}] 2 \mathcal{A}(\Delta(u_{1:3})) h(u_1 u_2) \sigma(du_{1:3}). \end{aligned}$$

First, we provide an upper bound for $a(n, \rho)$. Since $B(z, r) \cap C^{\varepsilon, \rho}(v) \neq \emptyset$ we have $z \in v \oplus [-\frac{3}{4} - \frac{\varepsilon_{\rho}}{2}, \frac{3}{4} + \frac{\varepsilon_{\rho}}{2}]^2$. Dividing the square $v \oplus [-\frac{3}{4} - \frac{\varepsilon_{\rho}}{2}, \frac{3}{4} + \frac{\varepsilon_{\rho}}{2}]^2$ into four quadrants of equal size, it follows that

$$\begin{aligned}
a(n, \rho) &\leq \frac{1}{2} 4n^3 \int_0^{\frac{3}{4} + \frac{\varepsilon_\rho}{2}} \int_0^{\frac{3}{4} + \frac{\varepsilon_\rho}{2}} \int_0^\infty e^{-n\pi r^2} r^4 dr dy_z dx_z \\
&= 2n^3 \left(\frac{3}{4} + \frac{\varepsilon_\rho}{2} \right)^2 \frac{3}{8\pi^2 n^{\frac{5}{2}}}. \tag{Eq. (13)}
\end{aligned} \tag{11}$$

Secondly, to provide an upper bound for $b(\rho, \kappa)$, we write

$$u_{1:3} := u(\beta_{1:3}) := (u(\beta_1), u(\beta_2), u(\beta_3))$$

with $u(\beta_i) = (\cos \beta_i, \sin \beta_i)$. Up to the line symmetry w.r.t. the y -axis, we impose that $\beta_3 \in [\frac{\pi}{2}, \frac{3\pi}{2}]$. Up to the line symmetry w.r.t. the x -axis, we also impose that $y_{u(\beta_2)} \geq y_{u(\beta_3)}$, i.e. $\beta_2 \in [\pi - \beta_3, \beta_3]$. Besides, $u_1 \in C(0, 1) \cap C(\beta_2)$, where $C(0, 1)$ is the unit circle and where $C(\beta_2)$ is the half-cone generated on the left of $u(\beta_2)$ by the x -axis, with vertex $u(\beta_2)$ and with angle $2\alpha_{\rho, \kappa}$, i.e.

$$C(\beta_2) := u(\beta_2) + \{(r \cos \gamma, r \sin \gamma) : r \geq 0, \gamma \in [\pi - \alpha_{\rho, \kappa}, \pi + \alpha_{\rho, \kappa}]\}.$$

We discuss four cases by splitting the domain of integration $[\pi - \beta_3, \beta_3]$ of β_2 as follows (see Figure 9):

1. If $\beta_2 \in [\pi - \beta_3, \frac{\pi}{2}]$, we have $\beta_1 \in [\pi - \beta_2 - 2\alpha_{\rho, \kappa}, \pi - \beta_2 + 2\alpha_{\rho, \kappa}]$ (Figure 9-left).
2. If $\beta_2 \in [\frac{\pi}{2}, \frac{\pi}{2} + \alpha_{\rho, \kappa}]$, the length of $C(0, 1) \cap C(\beta_2)$ is maximal when $\beta_2 = \frac{\pi}{2}$, so that $\beta_1 \in [\frac{\pi}{2}, \frac{\pi}{2} + 2\alpha_{\rho, \kappa}]$. Besides, the area of the triangle $\Delta(u(\beta_{1:3}))$ is less than $2\alpha_{\rho, \kappa}$ and $h(u(\beta_1)u(\beta_2))$ is also less than $2\alpha_{\rho, \kappa}$ (Figure 9-center).
3. If $\beta_2 \in [\frac{\pi}{2} + \alpha_{\rho, \kappa}, \frac{3\pi}{2} - \alpha_{\rho, \kappa}]$, we have $C(0, 1) \cap C(\beta_2) = \emptyset$.
4. If $\beta_2 \in [\frac{3\pi}{2} - \alpha_{\rho, \kappa}, \beta_3]$, with $\beta_3 > \frac{3\pi}{2} - \alpha_{\rho, \kappa}$, the length of $C(0, 1) \cap C(\beta_2)$ is maximal when $\beta_2 = \frac{3\pi}{2}$, so that $\beta_1 \in [\frac{3\pi}{2} - 2\alpha_{\rho, \kappa}, \frac{\pi}{2}]$. Besides, the area of the triangle $\Delta(u(\beta_{1:3}))$ is less than $2\alpha_{\rho, \kappa}$ and $h(u(\beta_1)u(\beta_2))$ is also less than $2\alpha_{\rho, \kappa}$ (Figure 9-left).

It follows that

$$\begin{aligned}
b(\rho, \kappa) &\leq 4 \int_{\frac{\pi}{2}}^{\frac{3\pi}{2}} \int_{\pi - \beta_3}^{\frac{\pi}{2}} \int_{\pi - \beta_2 - 2\alpha_{\rho, \kappa}}^{\pi - \beta_2 + 2\alpha_{\rho, \kappa}} 2\mathcal{A}(\Delta(u(\beta_{1:3}))) h(u(\beta_1)u(\beta_2)) d\beta_1 d\beta_2 d\beta_3 \\
&\quad + 16\pi\alpha_{\rho, \kappa}^4. \tag{1st case} \\
&\quad \tag{2nd & 4th cases}
\end{aligned}$$

Moreover, we know that

$$2\mathcal{A}(\Delta(u(\beta_{1:3}))) = \begin{pmatrix} 1 & 1 & 1 \\ \cos \beta_1 & \cos \beta_2 & \cos \beta_3 \\ \sin \beta_1 & \sin \beta_2 & \sin \beta_3 \end{pmatrix} \quad \text{and} \quad h(u(\beta_1)u(\beta_2)) = \cos \beta_1 - \cos \beta_2.$$

This gives

$$\begin{aligned}
b(\rho, \kappa) &\leq \frac{256}{9} \cos^3 \alpha_{\rho, \kappa} \sin \alpha_{\rho, \kappa} + \frac{128}{3} \cos \alpha_{\rho, \kappa} \sin \alpha_{\rho, \kappa} + \frac{128}{3} \alpha_{\rho, \kappa} + 16\pi\alpha_{\rho, \kappa}^4 \\
&\leq \frac{1024}{9} \alpha_{\rho, \kappa}. \tag{Eq. (23)}
\end{aligned}$$

This together with (10), (11) and the fact that $\mathbb{E} [L_{\varepsilon_\rho, \alpha_{\rho, \kappa}, \kappa}(v) \mathbb{1}_{[\mathcal{I}_{\varepsilon_\rho}(v)]}] \leq a(n, \rho) \times b(\rho, \kappa)$ with $\varepsilon_\rho = \sqrt{\rho}\sqrt{\rho+2}$ and $\alpha_{\rho, \kappa} = \sqrt{2\frac{\kappa}{\kappa-1}\rho}$, implies that

$$\begin{aligned} \mathbb{P} [\mathcal{I}_{\varepsilon_\rho}(v)] \mathbb{P} \left[\mathcal{H}'_{\varepsilon_\rho, \alpha_{\rho, \kappa}, \kappa}(v) \middle| \mathcal{I}_{\varepsilon_\rho}(v) \right] \\ \leq \kappa \cdot 2n^3 \left(\frac{3}{4} + \frac{\sqrt{\rho}\sqrt{\rho+2}}{2} \right)^2 \frac{3}{8\pi^2 n^{\frac{5}{2}}} \cdot \frac{1024}{9} \cdot \sqrt{2\frac{\kappa}{\kappa-1}\rho} \\ = 2 \cdot \frac{3}{8\pi^2} \frac{1024}{9} \sqrt{2} \left(\frac{3}{4} + \frac{\sqrt{\rho}\sqrt{\rho+2}}{2} \right)^2 \sqrt{\frac{\kappa^3}{\kappa-1}} \sqrt{\rho n} \\ \leq 31.76 \left(\frac{3}{4} + \frac{\sqrt{\rho}\sqrt{\rho+2}}{2} \right)^2 \sqrt{\rho n}. \end{aligned}$$

In the last line, we have taken $\kappa = \frac{3}{2}$ since it is the value of κ which minimizes $\frac{\kappa^3}{\kappa-1}$. The condition $\frac{\kappa}{\kappa-1}\rho < \frac{\pi^2}{8}$ is satisfied since $\rho < \frac{\pi^2}{24} \simeq 0.4$ by assumption. \square

Proof of Proposition 15. This is a direct consequence of Lemmas 17, 18 and 19 and the fact that

$$\mathbb{P} [\neg \mathcal{I}_{\varepsilon_\rho}(v) \vee \mathcal{H}_\rho(v)] \leq \mathbb{P} [\neg \mathcal{I}_{\varepsilon_\rho}(v)] + \mathbb{P} [\mathcal{I}_{\varepsilon_\rho}(v)] \mathbb{P} \left[\mathcal{H}'_{\varepsilon_\rho, \alpha_{\rho, \kappa}, \kappa}(v) \middle| \mathcal{I}_{\varepsilon_\rho}(v) \right]$$

The assumption $\rho < 4 \cdot 10^{-6}$ ensures that $\varepsilon_\rho < \frac{1}{700}$ in Lemma 18 and $\rho < 0.4$ in Lemma 19. \square

5.5 Wrap-up

Proof of Theorem 1. It follows from Lemma 14 that

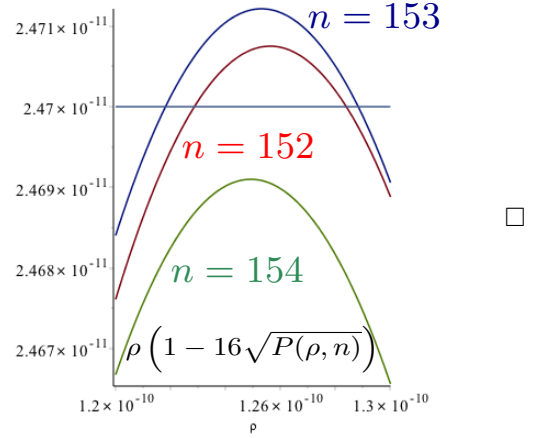
$$\begin{aligned} \mathbb{P} [\ell(SP_X) \leq k + \rho(k - 16k\sqrt{p})] &\leq \mathbb{P} \left[\max_{c \in \text{Colors}} \#\mathcal{H}(\mathbf{A}_{(c)}(SP_X)) \geq 4k\sqrt{p} \right] \\ &\leq \sum_{c \in \text{Colors}} \mathbb{P} [\#\mathcal{H}(\mathbf{A}_{(c)}(SP_X)) \geq 4k\sqrt{p}]. \end{aligned}$$

To bound the right-hand side, we apply Proposition 13 to the family of events $\mathcal{Y} := (Y_v)_{v \in \mathbb{Z}^2}$, where $Y_v := \mathcal{H}_\rho(v) \vee \neg \mathcal{I}_{\varepsilon_\rho}(v)$. Notice that for any color c , the events $(Y_v)_{v \in \mathbb{Z}_{s,t}^{2,(c)}}$ are independent: this comes from the fact that the event $\mathcal{H}_\rho(v) \vee \neg \mathcal{I}_{\varepsilon_\rho}(v)$ is $\sigma(X_n \cap C_2(v))$ measurable and the fact that $C_2(v) \cap C_2(w) = \emptyset$ when $v \neq w \in \mathbb{Z}_{s,t}^{2,(c)}$. Moreover, for any $v \in \mathbb{Z}_{s,t}^{2,(c)}$, the probability $p := \mathbb{P} [\mathcal{H}_\rho(v) \vee \neg \mathcal{I}_{\varepsilon_\rho}(v)]$ does not depend on v . Besides, to apply Proposition 13, we have to choose ρ and n in such a way that $p \leq 0.01$. Provided that such a condition is satisfied and that $\rho \leq 4 \cdot 10^{-6}$, it follows from Proposition 13 and Proposition 15 that

$$\mathbb{P} [\ell(SP_X) \leq k + \rho \left(1 - 16\sqrt{P(\rho, n)} \right) k] = O(k^{-1/2}).$$

To minimize $\rho \left(1 - 16\sqrt{P(\rho, n)}\right)$, we choose $\rho = 1.25 \cdot 10^{-10}$ and $n = 153$. Then we have $\rho < 4 \cdot 10^{-6}$ and $p \leq P(\rho, n) \simeq 0.0025 < 0.01$, so that the assumptions of Propositions 13 and 15 are satisfied. This concludes the proof of Theorem 1 since

$$\left(1 - 16\sqrt{P(\rho, n)}\right) \geq 2.47 \cdot 10^{-11}.$$



6 Simulations

We give below experimental values, which depend on the intensity n , for the expected length and the number of edges of the paths considered in this paper. We also experiment a third path, described below:

Greedy constructed Path GP_X : we define such a path, starting in s , by induction. Let $(T_i)_{0 \leq i \leq k}$ be the family of triangles in $\text{Del}(X)$ whose interior intersects $[s, t]$ and ordered from the left to the right. Let w be the last vertex inserted in the path and let i be the largest value such that $w \in T_i$. Then the edge of T_i incident to w which minimizes the angle with respect to the x -axis is added to the path (see Figure 2).

The code for these simulations is written with CGAL [6] and is available with this paper. Figure 10 and Table 1 give estimates of the expectations and of the standard deviations for the lengths and for the cardinalities of the paths UP_X , GP_X and SP_X . These estimates are based on 100 trials of Poisson point processes with intensity $n = 10$ millions. In particular, Propositions 6 and 7 are confirmed by our experiments. The correct value for $\mathbb{E}[\ell(SP_X)]$ is about 1.04 and the path GP_X , using simple trick to improve on UP_X , gives a path significantly shorter than UP_X . We also give experimental values for the straight walk SW_X .

path P	$\mathbb{E}[\ell(P)]$	$\sigma(\ell(P))$	$\frac{\mathbb{E}[\text{Card}(P)]}{\sqrt{n}}$	$\frac{\sigma(\text{Card}(P))}{\sqrt{n}}$
SW_X			2.1602	0.0154
UP_X	1.1826	0.0053	1.0804	0.0102
GP_X	1.1074	0.0036	1.0062	0.0084
SP_X	1.0401	0.0004	0.9249	0.0080

Table 1: Experimental values for SW_X , UP_X , GP_X and SP_X

Several illustrations of the paths UP_X , GP_X and SP_X are depicted in Figure 11 for various intensities.

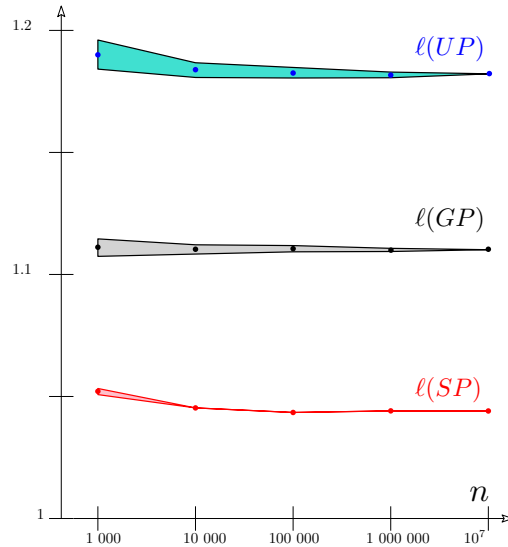


Figure 10: Experimental evaluations of $\mathbb{E}[\ell(SP_X)]$, $\mathbb{E}[\ell(GP_X)]$, and $\mathbb{E}[\ell(UP_X)]$ for various intensities with $\|s - t\| = 1$. The width of the drawing is the standard deviation.

7 Conclusion

We have provided a non-trivial lower bound for the inferior limit of the expectation of the stretch factor between two points s and t in $Del(X_n \cup \{s, t\})$ where X_n is an homogeneous Poisson point process when the intensity goes to infinity. The main difficulty is that we have absolutely no information on the exact location of the shortest path. Our lower bound for ρ is far from being tight since the experimental value is much larger. Although several constants in our proof can be improved a little bit, this scheme of proof can only give lower bounds which are far from optimal. Indeed, the first point where our evaluation is quite crude is the approximation of the Horizontality Property by the Weak Horizontality Property. Actually, a better upper bound for $\mathbb{P}[\mathcal{H}_\rho(v)]$ should widely improve ρ and an explicit lower bound for $\mathbb{P}[\mathcal{H}_\rho(v)]$ yields to a more precise evaluation of the convergence. Another point where we widely under-evaluate ρ comes from the fact that we use approximation by animals. Actually, a bad situation (when the shortest path is very short) corresponds to an animal with many pixels with a strong horizontality property. However, the converse is clearly not true. Thus we believe that the proof of a tight constant necessitates other techniques.

Another question raised by the paper is to prove that the limit of the expectation of the stretch factor exists. One of the underlying difficulties is to show that the function $k \mapsto \mathbb{E}[\ell(SP_X)]$, with $X = X_n \cup \{(0, 0), (k, 0)\}$ and $k \in \mathbb{R}_+$, is continuous and subadditive. It appears that these properties are not trivial. Indeed, conditioning by the fact that an intermediate point in $[s, t]$ belongs to the shortest path can increase or decrease the length of the shortest path in distribution. We hope, in a future work, to deal with these properties and to prove the existence of the limit.

Acknowledgements

The authors thanks David Coeurjolly for pointing us ref [14] for Lemma 10, and Louis Noizet for

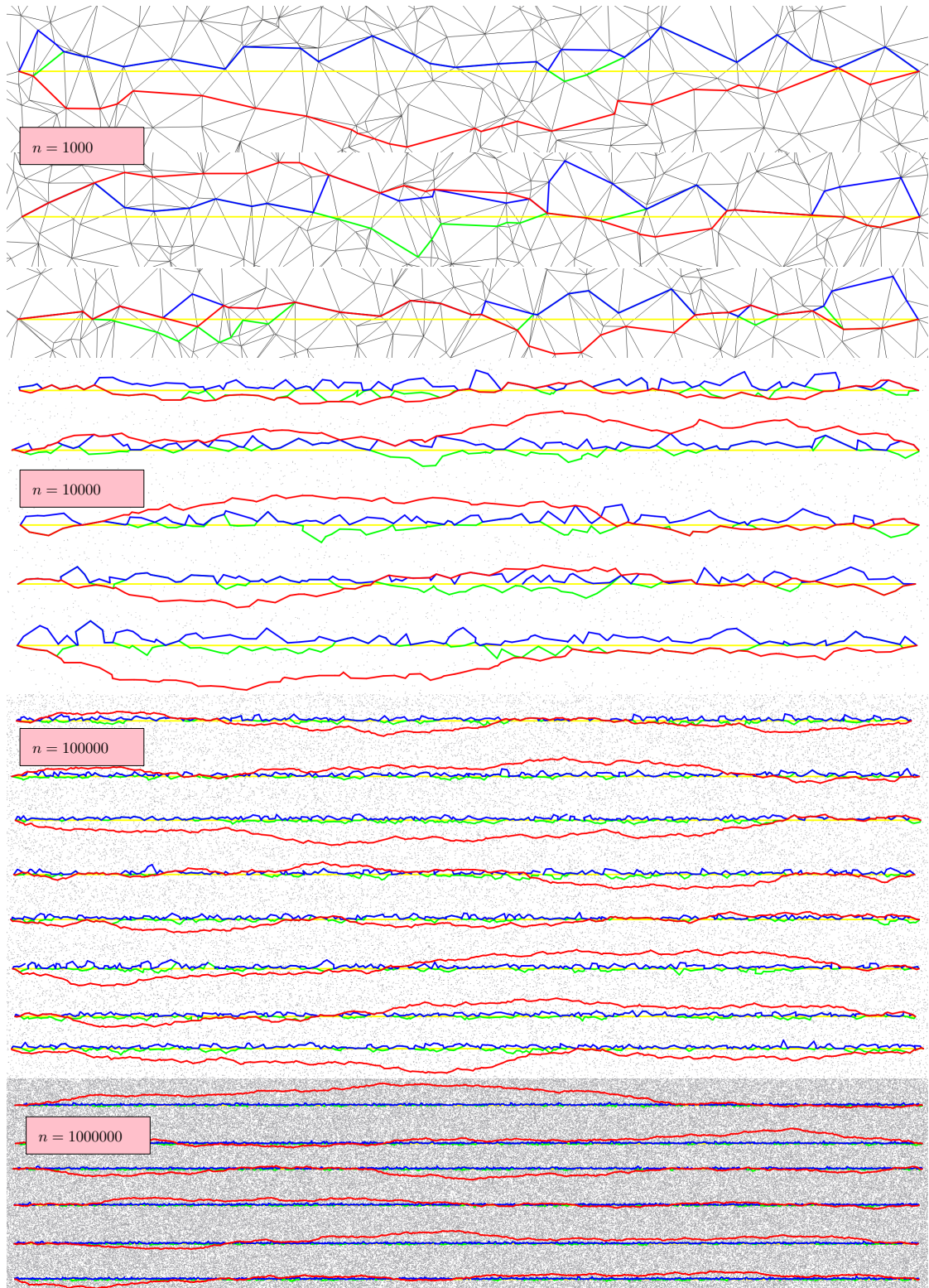


Figure 11: Several trials with intensity from $n = 1000$ to $n = 1$ million. The paths UP_X , GP_X , and SP_X are colored in blue, green, and red respectively and the line segment $[s, t]$ is colored in yellow.

discussions about the definition of UP_X .

References

- [1] Franz Aurenhammer, Rolf Klein, Der-Tsai Lee, and Rolf Klein, *Voronoi diagrams and Delaunay triangulations*, vol. 8, World Scientific, 2013. MR 3186045
- [2] François Baccelli, Konstantin Tchoumatchenko, and Sergei Zuyev, *Markov paths on the Poisson-Delaunay graph with applications to routing in mobile networks*, Adv. in Appl. Probab. **32** (2000), no. 1, 1–18. MR 1765174
- [3] Prosenjit Bose and Luc Devroye, *On the stabbing number of a random Delaunay triangulation*, Computational Geometry: Theory and Applications **36** (2006), 89–105. MR 2278009
- [4] Prosenjit Bose and Pat Morin, *Online routing in triangulations*, SIAM Journal on Computing **33** (2004), 937–951. MR 2065340
- [5] Frédéric Cazals and Joachim Giesen, *Delaunay triangulation based surface reconstruction*, Effective computational geometry for curves and surfaces, Springer, 2006, hal:inria-00070610, pp. 231–276.
- [6] *Computational Geometry Algorithms Library*, <http://www.cgal.org>.
- [7] Nicolas Chenavier and Olivier Devillers, *Stretch factor of long paths in a planar Poisson-Delaunay triangulation*, Research report, INRIA, 2016, Note to reviewer: we will make supplementary data available in HAL repository (unless EJP can host these data).
- [8] Siu-Wing Cheng, Tamal K Dey, and Jonathan Shewchuk, *Delaunay mesh generation*, CRC Press, 2012. MR 3156288
- [9] J Theodore Cox, Alberto Gandolfi, Philip S Griffin, and Harry Kesten, *Greedy lattice animals I: Upper bounds*, The Annals of Applied Probability (1993), 1151–1169. MR 1241039
- [10] Olivier Devillers and Ross Hemsley, *The worst visibility walk in a random Delaunay triangulation is $O(\sqrt{n})$* , Research Report 8792, INRIA, October 2015, hal-01216212.
- [11] Olivier Devillers, Sylvain Pion, and Monique Teillaud, *Walking in a triangulation*, Internat. J. Found. Comput. Sci. **13** (2002), 181–199. MR 1895778
- [12] Luc Devroye, Christophe Lemaire, and Jean-Michel Moreau, *Expected time analysis for Delaunay point location*, Computational Geometry: Theory and Applications **29** (2004), 61–89. MR 2082208
- [13] David P. Dobkin, Steven J. Friedman, and Kenneth J. Supowit, *Delaunay graphs are almost as good as complete graphs*, Discrete Comput. Geom. **5** (1990), 399–407. MR 1043722
- [14] Yan Gerard, Antoine Vacavant, and Jean-Marie Favreau, *Tight bounds in the quadtree complexity theorem and the maximal number of pixels crossed by a curve of given length*, Theoretical Computer Science (2015), 41–55. MR 3478914
- [15] Christian Hirsch, David Neuhaüser, and Volker Schmidt, *Moderate deviations for shortest-path lengths on random segment process*, 2016.

- [16] J. Mark Keil and Carl A. Gutwin, *The Delaunay triangulation closely approximates the complete Euclidean graph*, Proc. 1st Workshop Algorithms Data Struct., Lecture Notes Comput. Sci., vol. 382, Springer-Verlag, 1989, doi:10.1007/3-540-51542-9_6, pp. 47–56.
- [17] Rolf Schneider and Wolfgang Weil, *Stochastic and integral geometry*, Probability and Its Applications, Springer, 2008. MR 2455326
- [18] Ge Xia, *The stretch factor of the Delaunay triangulation is less than 1.998*, SIAM J. Comput. **42** (2013), 1620–1659. MR 3082502
- [19] Ge Xia and Liang Zhang, *Toward the tight bound of the stretch factor of Delaunay triangulations*, Proceedings 23th Canadian Conference on Computational Geometry, 2011, cccg.ca.

A Proof for the variance of UP_X

Proof of Proposition 8. According to Proposition 7 and the fact that $\mathbb{E}[\ell(UP_X)] = \mathbb{E}[L_{X_n}] + O\left(n^{-\frac{1}{2}}\right)$, where $X = X_n \cup \{s, t\}$ and $s = (0, 0)$, $t = (1, 0)$, it is enough to show that $\mathbb{E}[L_{X_n}^2] = \left(\frac{35}{3\pi^2}\right)^2 + O\left(n^{-\frac{1}{2}}\right)$.

Thanks to (5), we have $\mathbb{E}[L_{X_n}^2] = \mathbb{E}\left[\left(\sum_{p_1 \neq \dots \neq p_3 \in X_n^3} \ell_{X_n}(p_{1:3})\right)^2\right]$. To estimate the right-hand side, we will develop the terms inside the sum by discussing the number of common vertices between two triangles. To do it, we first give some notation. For each $0 \leq l \leq 2$, we denote by $\mathcal{S}_l \subset \{1 : 3 + l\}^3$ the set:

$$\mathcal{S}_l := \{(i_1, i_2, i_3) \in \{1 : 3 + l\}^3 : \text{Card}(\{i_1, i_2, i_3\} \cap \{1, 2, 3\}) = 3 - l\}.$$

Given a $(3 + l)$ -tuple of points $p_{1:3+l}$, we can associate a family of couple of triangles as follows. The first triangle is $\Delta(p_{1:3})$ and the second one is any triangle of the form $\Delta(p_{i_1} p_{i_2} p_{i_3})$ such that $(i_1, i_2, i_3) \in \mathcal{S}_l$. In particular, when $l = 0$, we have $\mathcal{S}_0 = \{1, 2, 3\}^3$ and $\Delta(p_{i_1} p_{i_2} p_{i_3}) = \Delta(p_{1:3})$. Notice that the term l is the number of vertices of the triangle $\Delta(p_{i_1} p_{i_2} p_{i_3})$ which are not vertices of the triangle $\Delta(p_{1:3})$. By developing the sum associated with L_{X_n} , we get

$$L_{X_n}^2 = \sum_{p_1 \neq \dots \neq p_6 \in X_n^6} l_{X_n}(p_{1:3}) l_{X_n}(p_{4:6}) + \sum_{l=0}^2 \sum_{(i_1, i_2, i_3) \in \mathcal{S}_l} \sum_{p_1 \neq \dots \neq p_{3+l} \in X_n^{3+l}} l_{X_n}(p_{1:3}) l_{X_n}(p_{i_1} p_{i_2} p_{i_3}).$$

As a first step, we show that

$$\mathbb{E}\left[\sum_{p_1 \neq \dots \neq p_6 \in X_n^6} l_{X_n}(p_{1:3}) l_{X_n}(p_{4:6})\right] = \left(\frac{35}{3\pi^2}\right)^2 + O\left(n^{-\frac{1}{2}}\right).$$

In the same spirit as in the proof of Proposition 7, we apply the Slivnyak-Mecke and Blaschke-Petkantschin fomulas. It follows that

$$\begin{aligned} \mathbb{E}\left[\sum_{(p_1 \neq \dots \neq p_6) \in X_n^6} l_{X_n}(p_{1:3}) l_{X_n}(p_{4:6})\right] &= n^6 \cdot \int_{(\mathbb{R}^2)^2} \int_{\mathbb{R}_+^2} \int_{(\mathbb{S}^3)^2} e^{-n \mathcal{A}(B(z,r) \cup B(z',r'))} \\ &\quad \times \mathbb{1}_{[z+ru_{1:3} \in E^+]} \mathbb{1}_{[z'+ru'_{1:3} \in E^+]} r^4 r'^4 \|u_2 - u_1\| \cdot \|u'_2 - u'_1\| \\ &\quad \times \mathcal{A}(\Delta(u_{1:3})) \mathcal{A}(\Delta(u'_{1:3})) \sigma(du_{1:3}) \sigma(du'_{1:3}) dr dr' dz dz'. \end{aligned}$$

Rewriting the exponential term in the integrand as

$$e^{-n \mathcal{A}(B(z,r) \cup B(z',r'))} = e^{-n\pi(r^2+r'^2)} + \left(e^{-n \mathcal{A}(B(z,r) \cup B(z',r'))} - e^{-n\pi(r^2+r'^2)}\right)$$

and applying Fubini's theorem, we deduce from (6) that

$$\mathbb{E}\left[\sum_{(p_1 \neq \dots \neq p_6) \in X_n^6} l_{X_n}(p_{1:3}) l_{X_n}(p_{4:6})\right] = (\mathbb{E}[L_{X_n}])^2 + r_n, \quad (12)$$

where

$$r_n := 2n^6 \cdot \int_{(\mathbb{R}^2)^2} \int_{\mathbb{R}_+^2} \int_{(\mathbb{S}^3)^2} \left(e^{-n\mathcal{A}(B(z,r) \cup B(z',r'))} - e^{-n\pi(r^2+r'^2)} \right) \\ \times \mathbb{1}_{[z+ru_{1:3} \in E^+]} \mathbb{1}_{[z'+ru'_{1:3} \in E^+]} r^4 r'^4 \|u_2 - u_1\| \cdot \|u'_2 - u'_1\| \mathcal{A}(\Delta(u_{1:3})) \\ \times \mathcal{A}(\Delta(u'_{1:3})) \mathbb{1}_{[B(z,r) \cap B(z',r') \neq \emptyset]} \mathbb{1}_{[r' \leq r]} \sigma(du_{1:3}) \sigma(du'_{1:3}) dz dz' dr dr'.$$

Notice that in the integrand of the rest r_n , we have added two indicator functions. The first one deals with the event $\{B(z,r) \cap B(z',r') \neq \emptyset\}$: this comes from the fact that, on the complement of this event, the integrand appearing in r_n equals 0 since $\mathcal{A}(B(z,r) \cup B(z',r')) = \pi(r^2 + r'^2)$. The second one concerns the event $r' \leq r$: by symmetry, this explains why we have added a constant 2 on the left of term n^6 . Besides, for the first term of the right-hand side in (12), we have $(\mathbb{E}[L_{X_n}])^2 = \left(\frac{35}{3\pi^2}\right)^2 + O\left(n^{-\frac{1}{2}}\right)$ according to Proposition 7. To deal with second term of the right-hand side in (12), we bound the terms appearing in the integrand as follows: first, we use the fact that $e^{-n\mathcal{A}(B(z,r) \cup B(z',r'))} - e^{-n\pi(r^2+r'^2)} \leq e^{-n\pi r^2}$ with $r' \leq r$. Secondly, for each $v_{1:3} \in \mathbb{S}^3$, we bound $\|v_2 - v_1\| \mathcal{A}(\Delta(v_{1:3}))$ by a constant, by taking successively $v_{1:3} = u_{1:3}$ and $v_{1:3} = u'_{1:3}$. Thirdly, as in the proof of Proposition 7, we notice that $z \in [0, 1] \times [-r, r]$ since $z + ru_{1:3} \in E^+$. Finally, we also use the fact that $\mathbb{1}_{[B(z,r) \cap B(z',r') \neq \emptyset]} \leq \mathbb{1}_{[z' \in B(z, 2r)]}$. It follows that

$$r_n \leq cn^6 \cdot \int_{(\mathbb{R}^2)^2} \int_{\mathbb{R}_+^2} e^{-n\pi r^2} r^4 r'^4 \mathbb{1}_{[z \in [0,1] \times [-r,r]]} \mathbb{1}_{[z' \in B(z, 2r)]} \mathbb{1}_{[r' \leq r]} dz dz' dr dr'.$$

Integrating successively over $r' \leq r$, $z' \in B(z, 2r)$ and $z \in [0, 1] \times [-r, r]$, we get

$$r_n \leq c \cdot n^6 \int_{\mathbb{R}_+} r^{12} e^{-n\pi r^2} dr = O\left(n^{-\frac{1}{2}}\right). \quad \text{Eq. (19)}$$

As a second step, we show that

$$\mathbb{E} \left[\sum_{p_1 \neq \dots, p_{3+l} \in X_n^{3+l}} l_{X_n}(p_{1:3}) l_{X_n}(p_{i_1}, p_{i_2}, p_{i_3}) \right] = O\left(n^{-\frac{1}{2}}\right)$$

for any $0 \leq l \leq 2$ and $(i_1, i_2, i_3) \in \mathcal{S}_l$. In this case, the triangles $\Delta(p_{1:3})$ and $\Delta(p_{i_1}, p_{i_2}, p_{i_3})$ share at less one vertex in common. By symmetry, we have

$$\sum_{p_1 \neq \dots, p_{3+l} \in X_n^{3+l}} l_{X_n}(p_{1:3}) l_{X_n}(p_{i_1}, p_{i_2}, p_{i_3}) \\ = 2 \cdot \sum_{p_1 \neq \dots, p_{3+l} \in X_n^{3+l}} l_{X_n}(p_{1:3}) l_{X_n}(p_{i_1}, p_{i_2}, p_{i_3}) \mathbb{1}_{[R(p_{i_1}, p_{i_2}, p_{i_3}) \leq R(p_{1:3})]}$$

Assuming that $R(p_{i_1}, p_{i_2}, p_{i_3}) \leq R(p_{1:3})$, we obtain that $l_{X_n}(p_{i_1}, p_{i_2}, p_{i_3}) \leq 2 \cdot R(p_{1:3})$. Moreover, we have $p_{i_1}, p_{i_2}, p_{i_3} \in 3B(p_{1:3})$ where $3B(p_{1:3})$ is the ball concentric with $B(p_{1:3})$ and radius three

times bigger. It follows that

$$\begin{aligned} \sum_{p_1 \neq \dots, 3+l} \in X_n^{3+l} l_{X_n}(p_{1:3}) l_{X_n}(p_{i_1}, p_{i_2}, p_{i_3}) \\ \leq c \cdot \sum_{p_1 \neq \dots, 3+l} \in X_n^{3+l} l_{X_n}(p_{1:3}) R(p_{1:3}) \mathbb{1}_{[R(p_{i_1}, p_{i_2}, p_{i_3}) \leq 3B(p_{1:3})]}. \end{aligned}$$

In the above equation, we have bounded the indicator function $\mathbb{1}_{[R(p_{i_1}, p_{i_2}, p_{i_3}) \leq R(p_{1:3})]}$ by 1. In the same spirit as above, we first apply the Slivnyak-Mecke formula. This gives

$$\begin{aligned} \mathbb{E} \left[\sum_{p_1 \neq \dots, 3+l} \in X_n^{3+l} l_{X_n}(p_{1:3}) l_{X_n}(p_{i_1}, p_{i_2}, p_{i_3}) \right] \\ \leq c \cdot n^{3+l} \int_{(\mathbb{R}^2)^3} \left(\int_{(\mathbb{R}^2)^l} \mathbb{1}_{[q_{1:l} \in (3B(p_{1:3}))^l]} dq_{1:l} \right) \mathbb{E} [l_{X_n \cup \{p_{1:3}\}}(p_{1:3})] R(p_{1:3}) dp_{1:3} \\ = c' \cdot n^{3+l} \int_{(\mathbb{R}^2)^3} \mathbb{E} [l_{X_n \cup \{p_{1:3}\}}(p_{1:3})] (R(p_{1:3}))^{1+2l} dp_{1:3}. \end{aligned}$$

It follows from the Blaschke-Petkantschin formula that

$$\begin{aligned} \mathbb{E} \left[\sum_{p_1 \neq \dots, 3+l} \in X_n^{3+l} l_{X_n}(p_{1:3}) l_{X_n}(p_{i_1}, p_{i_2}, p_{i_3}) \right] \leq c' \cdot n^{3+l} \int_{\mathbb{R}_+} \int_{\mathbb{R}^2} \int_{\mathbb{S}^3} e^{-n\pi r^2} \|u_2 - u_1\| r \\ \cdot \mathbb{1}_{[z + ru_{1:3} \in E^+]} \cdot r^{1+2l} \cdot 2 \mathcal{A}(\Delta(u_{1:3})) r^3 \sigma(du_{1:3}) dz dr. \end{aligned}$$

Since $z + ru_{1:3} \in E^+$ implies that $z \in [0, 1] \times [-r, r]$, we obtain by integrating over z and $u_{1:3}$ and using Equations (16), (17), and (18) that

$$\mathbb{E} \left[\sum_{p_1 \neq \dots, 3+l} \in X_n^{3+l} l_{X_n}(p_{1:3}) l_{X_n}(p_{i_1}, p_{i_2}, p_{i_3}) \right] \leq c'' \cdot n^{3+l} \int_{\mathbb{R}_+} e^{-n\pi r^2} r^{6+2l} dr = O\left(n^{-\frac{1}{2}}\right).$$

□

B Integrals

In this section, we provide values for several integrals which are often used in the paper. These integrals can be computed by using tedious classical computations. These computations are done with Maple (a Maple sheet is available with this paper).

$$\int_0^{\infty} e^{-n\pi r^2} r^4 dr = \frac{3}{8\pi^2 n^2 \sqrt{n}} \quad (13)$$

$$\int_0^{\infty} e^{-n\pi r^2} r^5 dr = \frac{1}{\pi^3 n^3} \quad (14)$$

$$\int_1^{\infty} e^{-n\pi r^2} r^5 dr = e^{-n\pi} \left(\frac{1}{2\pi n} + \frac{1}{\pi^2 n^2} + \frac{1}{\pi^3 n^3} \right) \quad (15)$$

$$\int_0^{\infty} e^{-n\pi r^2} r^6 dr = \frac{15}{16\pi^3 n^3 \sqrt{n}} \quad (16)$$

$$\int_0^{\infty} e^{-n\pi r^2} r^8 dr = \frac{105}{32\pi^4 n^4 \sqrt{n}} \quad (17)$$

$$\int_0^{\infty} e^{-n\pi r^2} r^{10} dr = \frac{945}{64\pi^5 n^5 \sqrt{n}} \quad (18)$$

$$\int_0^{\infty} e^{-n\pi r^2} r^{12} dr = \frac{10395}{128\pi^6 n^6 \sqrt{n}} \quad (19)$$

$$\begin{aligned} & \int_{[0,2\pi]^3} \left| \det \begin{pmatrix} 1 & 1 & 1 \\ \cos \beta_1 & \cos \beta_2 & \cos \beta_3 \\ \sin \beta_1 & \sin \beta_2 & \sin \beta_3 \end{pmatrix} \right| d\beta_{1:3} \\ &= 3! \int_0^{2\pi} \int_0^{\beta_3} \int_0^{\beta_2} \det \begin{pmatrix} 1 & 1 & 1 \\ \cos \beta_1 & \cos \beta_2 & \cos \beta_3 \\ \sin \beta_1 & \sin \beta_2 & \sin \beta_3 \end{pmatrix} d\beta_1 d\beta_2 d\beta_3 = 24\pi^2 \end{aligned} \quad (20)$$

$$\begin{aligned} & \int_{-1}^1 \int_{\pi+\arcsin h}^{2\pi-\arcsin h} \int_{-\arcsin h}^{\pi+\arcsin h} \int_{-\arcsin h}^{\pi+\arcsin h} \left| \det \begin{pmatrix} 1 & 1 & 1 \\ \cos \beta_1 & \cos \beta_2 & \cos \beta_3 \\ \sin \beta_1 & \sin \beta_2 & \sin \beta_3 \end{pmatrix} \right| d\beta_1 d\beta_2 d\beta_3 dh \\ &= 2 \int_{-1}^1 \int_{\pi+\arcsin h}^{2\pi-\arcsin h} \int_{-\arcsin h}^{\pi+\arcsin h} \int_{-\arcsin h}^{\beta_2} \det \begin{pmatrix} 1 & 1 & 1 \\ \cos \beta_1 & \cos \beta_2 & \cos \beta_3 \\ \sin \beta_1 & \sin \beta_2 & \sin \beta_3 \end{pmatrix} d\beta_1 d\beta_2 d\beta_3 dh \\ &= \frac{512}{9} \end{aligned} \quad (21)$$

$$\begin{aligned} & \int_{-1}^1 \int_{\pi+\arcsin h}^{2\pi-\arcsin h} \int_{-\arcsin h}^{\pi+\arcsin h} \int_{-\arcsin h}^{\beta_2} \det \begin{pmatrix} 1 & 1 & 1 \\ \cos \beta_1 & \cos \beta_2 & \cos \beta_3 \\ \sin \beta_1 & \sin \beta_2 & \sin \beta_3 \end{pmatrix} \\ & \quad \times 2 \sin \frac{\beta_2 - \beta_1}{2} d\beta_1 d\beta_2 d\beta_3 dh \\ &= \frac{35\pi}{3} \end{aligned} \quad (22)$$

$$\begin{aligned} & \int_{\frac{\pi}{2}}^{\frac{3\pi}{2}} \int_{\pi-\beta_3}^{\frac{\pi}{2}} \int_{\pi-\beta_2-2\alpha_{\rho,\kappa}}^{\pi-\beta_2+2\alpha_{\rho,\kappa}} \det \begin{pmatrix} 1 & 1 & 1 \\ \cos \beta_1 & \cos \beta_2 & \cos \beta_3 \\ \sin \beta_1 & \sin \beta_2 & \sin \beta_3 \end{pmatrix} (\cos \beta_1 - \cos \beta_2) d\beta_1 d\beta_2 d\beta_3 \\ &= \frac{64}{9} \cos^3 \alpha_{\rho,\kappa} \sin \alpha_{\rho,\kappa} + \frac{32}{3} \cos \alpha_{\rho,\kappa} \sin \alpha_{\rho,\kappa} + \frac{32}{3} \alpha_{\rho,\kappa} \end{aligned} \quad (23)$$

The Inria logo is written in a red, cursive script font. The letters are connected and have a slight shadow effect, giving it a three-dimensional appearance as if it's floating above a white surface.

Inria

**RESEARCH CENTRE
NANCY – GRAND EST**

615 rue du Jardin Botanique
CS20101
54603 Villers-lès-Nancy Cedex

Publisher
Inria
Domaine de Voluceau - Rocquencourt
BP 105 - 78153 Le Chesnay Cedex
inria.fr

ISSN 0249-6399